Interactive comment on “Intermediate water flows in the South West Pacific from OUTPACE and THOT Argo floats” by Simon Barbot et al.
Received and published: 23 April 2018

Response to : Anonymous Referee #1

The paper is constructed on float trajectories, dissolved oxygen data and HYCOM model simulations. Two really different topics are discussed with little link between the two. The first one: how eddy structures contribute to water mixing at intermediate depths close to Queensland, and the second one on characterizing wave structures between two intermediate jets in middle tropical Pacific. Little use is made of the float data for this second theme (and even for the first one), except for the trajectories. In particular, I don’t understand why T, S, and density of the floats are not used (in complement or to validate HYCOM simulations, granted that this simulation likely assimilates those data). Furthermore, I did not get fully convinced that the plane waves were observed for almost two whole years, or what the criteria used to determine one optimal couple (frequency, wavelength) really select. In some ways, nonetheless, some limitations of the approach used are reported in the discussion section. I was also expecting in this section a discussion (some hints) on processes that could favor the generation of waves at that period and latitude. . . A strong signal at 900m surprised me a little for a mode estimated with a thermocline at 200m. Could it be local instability around currents at intermediate depth (or further up in water column?), and maybe some frequency selection due to such dynamical processes, and the dispersive/propagative properties of Rossby waves in a horizontally-sheared environment. These are many elements missing that would contribute to make the paper valuable.
The paper also complements to some extent results discussed in earlier papers (Rousselet et al. 2016, 2017), at least for the first topic. Thus, I do not recommand that the paper be published, as constructed. It would probably be more valuable to focus in more depth on the second topic, so that the results provided that would be easier to assess.

As quoted by Moutin et al. (2017, preface of the special issue), "the goal of this special issue is to present the knowledge obtained concerning the functioning of WTSP ecosystems and associated biogeochemical cycles based on the datasets acquired during the OUTPACE experiment". It takes place along a 4000km zonal transect from the north of New Caledonia to the French Polynesia. As it is well known, the spatio-temporal domain of an oceanographic cruise is characterized by horizontal stirring generated by ocean circulation at the mesoscale, inducing strong variability in different parameters. Consequently, studying the relevant large-scale dynamics and its potential links to the ephemeral and local gradients due to mesoscale activity is essential to provide a broad overview of the observations, from the time of the cruise and beyond. In this long-term and large scale context, it is true that various physical processes could interplay. It is, in some way, the objectives of our study to document and to explain the processes that favor the generation of the observed data collected from a Lagrangian point of view (i.e., Argo floats). We agree that some elements were previously missing. We have taken care, with great attention, of the proposed suggestions in order to make a valuable manuscript, and hence have included references to earlier papers in both regions under consideration and additions in the proposed methodology. As the main results of the OUTPACE cruise are based on the full transect, and especially on the zonal large-scale gradient of biology and biogeochemistry of diazotroph organisms, we continue to believe that a dynamical study of the different regimes in the intermediate waters is highly relevant for this special issue. , We have also taken into account the editorial propositions and the very constructive suggestions on our approach. We sincerely thank the reviewer for his/her patient and careful reading. Details of our responses and additions to our original manuscript are described below.

Finally, the paper needs to be thoroughly edited. What follows are comments or suggestions for changes through the manuscript.
p.1, Line 20: ’place’ instead of ’replace’ Done
p.1, l. 23: replace ’complete’ by ’complement’ Done
statement, l. 1 of p. 2: statement was not introduced, but reads as a conclusion statement. Should be supported first by references of what can be done. This sentence would then conclude the paragraph. Done, the paragraph has become :
"Autonomous Argo floats are profilers parked at 1000 m depth and reaching the surface every 10 days, where they transmit their measurements and location (further information on the cycle of the different Argo floats we used is detailed in the next section).

Current speeds at the parking depth of the floats are then calculated, leading to horizontal gridded maps of velocities either global (Davis, 2005, Ollitrault and Rannou, 2013) or regional (Cravatte et al., 2012). Other approaches are developed in order to study the intermediate circulation, for example by taking into account the spreading of different float trajectories from a same position (Sevellec et al., 2017). Moreover, when Argo floats are BCG, on top of allowing the study of intermediate circulation, they provide measurements of biogeochemistry and biology parameters over the first thousand meters of the water column."

p. 2, L. 2: replace 'they' by 'there' Done

p. 2, l.13:'more deoxygeneated'. Better to write 'less oxygenated' (or 'low oxygen event') Done

p.2, l.14: 'longer branch'. . . implication is that water mass is 'older' based on its last contact to the surface, thus less ventilated? Longer 'path without ventilation' is more accurate, the sentence has been corrected and now is:

"The NVJ is older, in the sense that it originates from a longer path than the NCJ, since its last contact to the surface. Hence, without ventilation, the DOXY of the NVJ intermediate waters is lower than the NCJ DOXY.

p. 2, l. 26: 'highlighted' Done

p. 2, l. 33, and p.4, l.1:'place' instead of 'replace' Done

p. 3, last line: replace 'the studies float' by 'the floats in this study' Done

p. 4, l. 9: replace 'By memory, it begins. . .' by 'This cycles starts. . .' Done

p.4, l. 11:'like those. . .' by 'such as those. . .' Done

p. 4, l. 15: 'immersed' by 'deployed' Done

p. 4, l. 16:'point to them' by 'refer to them'. I think that this sentence should be rewritten Done, the sentence has become :

"Hereafter, we only use the three last digits of the float number to refer to them, i.e. float 656 refers to #6901656.

Presentation of the floats on page 4: I got lost, which are the floats that are Arvor and Argos-located, and which is the float (656, only? Is it a PROVBIO?) that is iridium located . To clarify that we have added the sentence :

"In this study, we use three PROVBIO floats using Iridium (656, 660 and 687) and two ARVOR floats using ARGOS (671 and 679)."

Then, a discussion argues that there is little influence of surface displacement on the intermediate depth current estimates. I thought that this was not negligible for the Argos-located floats, because of longer time spent at the surface. It would be good to explain what assumption is done and further arguments for why this is not an issue for the paper? It is true that ARVOR floats (due to longer times remaining at the surface for telecommunications) have greater sensitivity to surface currents than PROVBIO ones; see the table below that has been added to the article.

Table 1: Statistics for the different floats between surface and deep trajectories, the results are presented as 'mean $\pm$ std'.

Float	Type	Surface distance [km]	Deep distance [km]	Surface speed [cm/s]	Deep speed [cm/s]
656	PROVBIO	0.44 ± 0.23	17.32 ± 18.18	29.57 ± 15.83	4.30 ± 3.93
660	PROVBIO	0.35 ± 0.18	15.96 ± 9.28	25.77 ± 13.16	3.65 ± 1.87
671	ARVOR	6.08 ± 3.44	25.30 ± 14.04	28.37 ± 16.12	3.00 ± 1.67
679	ARVOR	4.84 ± 2.38	21.88 ± 12.17	22.44 ± 11.07	2.60 ± 1.45
687	PROVBIO	0.33 ± 0.19	8.54 ± 6.53	24.26 ± 13.20	3.66 ± 1.89

We have also replaced the sentence "After some verifications...deep displacement." by the paragraph :

"Table 1 shows the mean properties of displacements for each studied float. First, it highlights the differences in surface distances between PROVBIO and ARVOR floats. At the surface, ARVOR floats drift over a distance about 10 times greater than PROVBIO floats. This is due to the longer time they spent at the surface (6h for ARVOR floats and 24min for PROVBIOs). The ratio between deep and surface distances is a factor of 30 for PROVBIO floats and still 4 for ARVOR ones. Float 656 exhibits anomalously high standard deviation for its deep distance and deep speed. These high values, of the same order as the mean ones, are due to the period during which the float was grounded on the sea floor in the Queensland plateau. Otherwise we have concluded that surface displacements can be neglected compared to deep displacements without doubt for PROVBIO floats and with caution for ARVOR floats. Hence, when needed in the wave section, we will only use the former ones and consider that the trajectory dynamics are mainly due to deep circulation processes. The discussion of such considerations is thoroughly made by Ollitrault and Rannou (2013)."

p.5, I don't understand the title of section 2.2 The idea was to consider the trajectory as wave signature ("wave approach"). It should be clearer that way : "Wave characteristics from float trajectories"

p. 5, l.6: why include k_z in k (and thus in lambda), as trajectories are horizontal. . . (actually, zonal) We were explaining the decomposition in a very general case. We have suppressed this part and directly use « $k = k_{lon}$ » for a zonal case.

p. 5, l. 19: what is a 'half float wave'? (the terminology is rather vaguely defined in this chapter). We have replaced the sentence "we choose to determine...wave ones." by :

"we choose not to describe the complete float wave characteristics (T, λ) but their halves ($T/2$, $\lambda/2$). In practice, this means we measure time and distance from crest to trough (and so on) rather than from crest to crest, for each studied float (floats 660, 671, 679 and 687, Fig.2). Hence, it allows to have more estimates when incomplete cycles are present." The estimations of $\lambda/2$ are made from the position maps and the ones of $T/2$ from the float time series of latitude.

How is the estimate made, in an environment which is clearly not mono-chromatic? As explained in the text (p.5 l.14 of the first submitted version), because of the shortness of the time series with regard to the sampling frequency, we cannot perform a Fourier transform or a wavelet analysis. Hence we decided to try to describe the wave in the simplest way as a mono-chromatic wave.

Some of the presentation might be necessary, but it has long been presented in various papers (for example Flierl, 1981). We seem to be in the case of no 'trapping' of floats in eddies (surface-intensified signature versus drift at 1000-m); thus classical 'linear' approach. Since this article is proposed for publication in the OUTPACE Special Issue mainly composed of biogeochemistry articles, we made the choice to start the explanation of the methods with a very generic/basic framework without using the complete terminology used by Flierl (1981), which is harder to comprehend for non physical oceanographers. Nonetheless, we have added the reference to Flierl (1981) as well as part of his terminology. The first paragraph of section 2.2 has become :

"Here the objective is to find the characteristics of a single wave that could explain the float trajectories which represent both retrograde and prograde circulation (retrograde when Lagrangian motion is in the opposite direction as the wave propagation ; prograde when Lagrangian motion and wave propagation are in the same direction; as defined in Flierl, 1981). We have also added some diagnostics to characterize the best fitting wave. We have added a paragraph at the end of the section 2.2 :

"According to Flierl (1981), for each float, we can define

$$\varepsilon = \frac{u_0}{c} \tag{1}$$

where c is the phase speed of the wave ($c = \frac{\omega}{k}$). The sign of ε indicates the type of motion of the float (prograde or retrograde) and its amplitude compares the particle velocity to the wave speed." We have also added the results of this calculation at the end of Section 3.2.1. As mentioned in the results section (p.15 l.24 to 28 of the first submitted version) , we observed eddy structures in the velocity field of HYCOM but this hypothesis does not explain the entire 660 trajectory (only its beginning is influenced by an eddy). Moreover no eddy is present along the entire 687 trajectory. Furthermore, the dominance of deep distances over surface ones (see table above) does not induce to decouple surface signature versus deep drift. Indeed the trajectories of the floats are not shifted only during the surface periods of their cycles but mostly during their parking depth periods. Added to the general absence of eddies, we consider that all this suggests that the wave signature is present at this deep depth.

Not completely sure that I understand what is thought after. What is probably assumed is that one considers non-dispersive (and mono-chromatic, at least a dominance of one frequency) waves? This is sort of assumed by the approach. Yes, it is. That is why we had used the term "plane wave". We have tried to make it clearer substituting "Because of the zonal tendency...system of equations" by : "Because of the zonal tendency of the studied float trajectories (Fig. 2), we express a simple case of the current perturbations due to a homogeneous, monochromatic wave (hereafter plane wave propagation) with the following system of equations..."

Not sure why an inverse model approach is not feasible. It is not the choice that we made; but we have added it as another perspective in the last section : "Another approach could also be made with an inverse model."

Also, hard to see how quantitative is the approach with this J index. Maybe, this could be tested in the model simulations or in simulated fields made up from a superposition of plane waves over a sheared background, for example. Our approach is to test the hypothesis that one single wave could be responsible for these float trajectories. The approach of the J index is to get a first guess of what could be the characteristics of such wave. This could be confirmed/denied with a more complex study, inverse methods or study implying several waves/eddies. The improvement of the calculation and representation of J-index is described below.

p. 7, l. 8: two indices. . .' Done

p. 9, l.10: The last sentence is not clear. Is it the part of the trajectory after October 2016, or the whole trajectory. If this is the full trajectory, this sentence can be removed (which is what I guess from what follows). Indeed it is the full trajectory, we removed the last sentence.

p. 9, l.20: replace 'deoxygenation events' by 'low oxygen'. Deoxygenation refers to something else, and should be replaced throughout the paper by other words. Thank you for also pointing that to us; we did substitute D1 and D2 by O1 and O2.

p. 9, l. 22: there seems to be another low oxygen event between D1 and D2 (although less consistent vertically). Yes, but we chose to focus on the events which are below 140 μmol/kg (p.9 l.20) because, in this way, we can avoid other hypotheses explaining low DOXY (as strong primary production for example).

p. 9, l. 25: this seems rather hypothetical statement (NVJ is four degrees further north). What is the evidence for that in the two papers referred to? (afterwards, I saw Appendix B figure, and figure 5 that provides quite compelling evidence) The two papers refer to the NVJ intrusion on the NCJ pathway hypothesis ; we have added a reference to Figure 5b to justify this statement.

p. 11,figure 5: the southward currents in A are not that strong. Focus on A, and not on C2? We did focus on C2 : "Figure 5b clearly shows that the NVJ waters can be associated with C2 for instance." (p.11 l.11 of the first submitted version and p.11 l.21 of the revised version that will be transmitted as soon as requested)

Question is density in HYCOM comparable to float density at 300m ? (I expect that as the Argo data are assimilated in HYCOM. . .) We are confident in the HYCOM results as the NCODA system (Cummings, 2005; Cummings and Smedstad, 2014), that is used by the HYCOM model, assimilates available satellite altimeter observations, satellite and in situ SST as well as vertical temperature and salinity profiles (from XBTs, Argo floats and moored buoys). It should be noticed that the profiles from our Argo floats are flagged good or probably good, meaning that these data are likely considered by the re-analysis. A comparison of Argo data with HYCOM re-analysis is shown in Fig.C1,C2 and C3 (next pages). Since a detailed validation is not the purpose of the study, these figures have been added in an appendix of the article, and not in the main text. We add the following paragraph at the beginning of the Section 3.1.1 :

"In addition, we also expose the corresponding Argo profiles from HYCOM re-analyses in the Appendix C. As expected from a re-analyses that assimilates different measurements including Argo float data, the salinity and temperature are in good agreement with the float measurements."

p. 11, l. 12-14: I am not sure what this adds. I think that one could remove these two sentences. This was to exhibit the case of D1/01 but we agree that it does not add much to the article; we have removed the sentences.

p. 12, choice of the J-index. Why this metrics instead of other ones (after all, it is a way to normalize errors in simulating meridional trajectories). When summing the two floats, wouldn't it have been better to normalize the respective two with the variance of respective meridional displacements (p. 8). Thanks for this proposition. At first, we thought that this would also help to get a fit closer to the 660 trajectory. Nonetheless, it turns out that the normalization does not change the results (Figure J below). To show the J index quantitatively, we have changed the red dots of Figure 6B of the first submitted version, with the real value of J and hence also transformed the colorbar to its right to represent the normalized J scale (see below).

Fig. 7 on page 14 is rather interesting, but somehow I wonder whether the fit is much better for 687 than for 660 (in particular, for the first part, when the two floats are rather close-by)? As explained at the end of the results (p.15 l.24), the beginning of the 660 trajectory is influenced by an eddy and otherwise the rest of the trajectory is also more irregular than the 687 trajectory. The first perspective that we mention in the discussion (to consider a variation of the zonal background current) would probably allow to get a better fit (Fig.10).

p. 15, l. 1-4: the comment on striations in HYCOM being different. I don't fully understand the comment. It would suggest that the model is not fully appropriate to provide the circulation context. This was a simple observation. This difference could be due to the fact that HYCOM re-analysis figures only represent an instantaneous snapshot versus a more than 10-year mean for the figure of Ollitrault and Colin de Verdière (2014). A more complete study should compare the two approaches and their impact on striations, but it is not the purpose of our study and needs further investigations.

p. 15, l.12: 'such as on November 13th' Done

p. 15, l.13: replace 'globally' by 'usually' (and then again 'like' by 'such as' on lines 12 and 13) Done

p.15, l. 14: ambiguous sentence. Is the S (density) meridional gradient just near 900m depth, or do you select the value at 900m depth to illustrate the meridional gradient. Figure 9a shows a meridional gradient of salinity between 1200 m and 500 m depth, but the gradient that is being used in our study is the one at the parking depth of the float, so around 1000 m depth. To clarify, we have substituted the sentence "Meridional cross-sections...around 900 m" by :

"Meridional cross-sections of HYCOM re-analysis (Fig. 9a) show a salinity gradient in the intermediate waters, between 500 m and

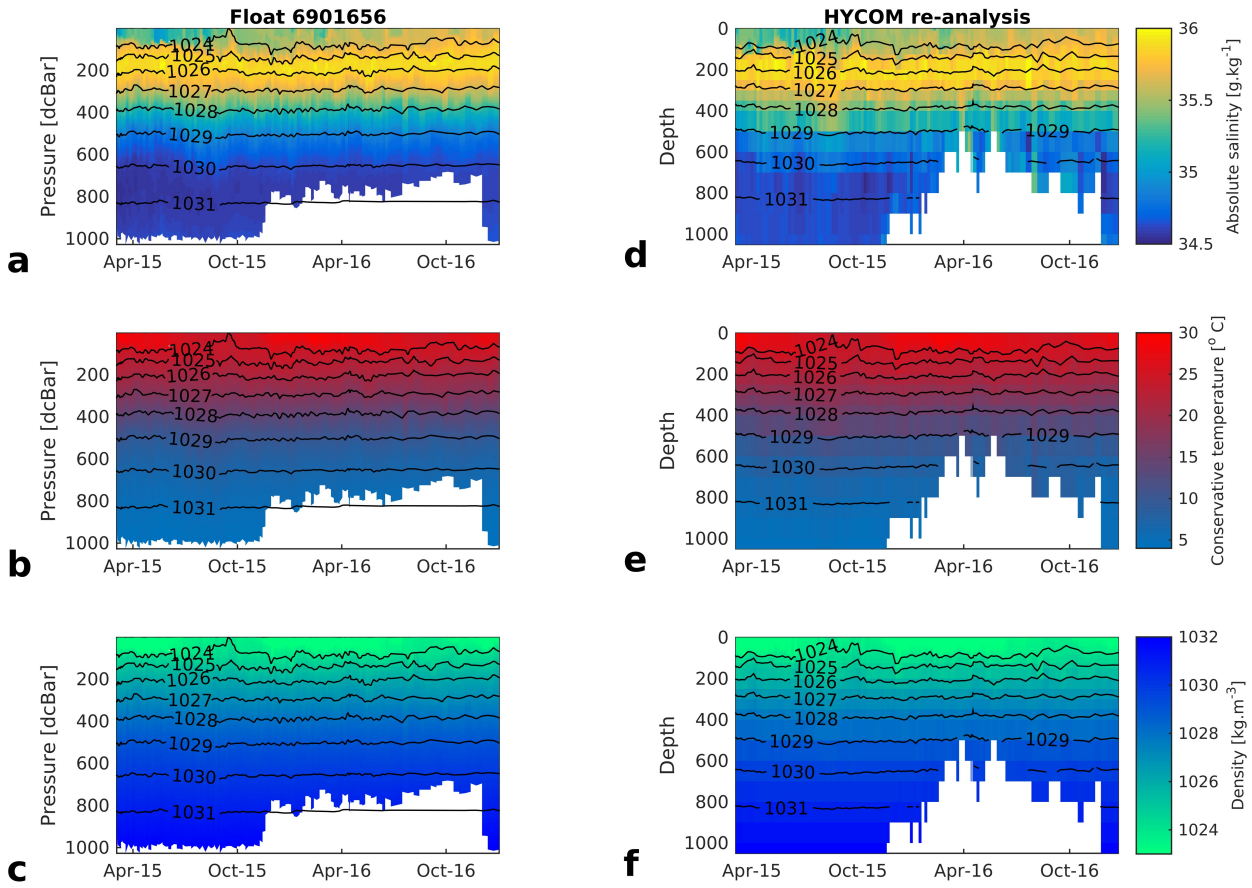

FIGURE C1 : Profiles of (left side) float 656 and (right side) corresponding data from HYCOM re-analysis over depth and time for (a,e) absolute salinity, (b,f) conservative temperature and (c,g) density. Every colored point corresponds to a measurement. The black lines indicate the isopycnals from 1024 to 1031 kg.m^{-3}.

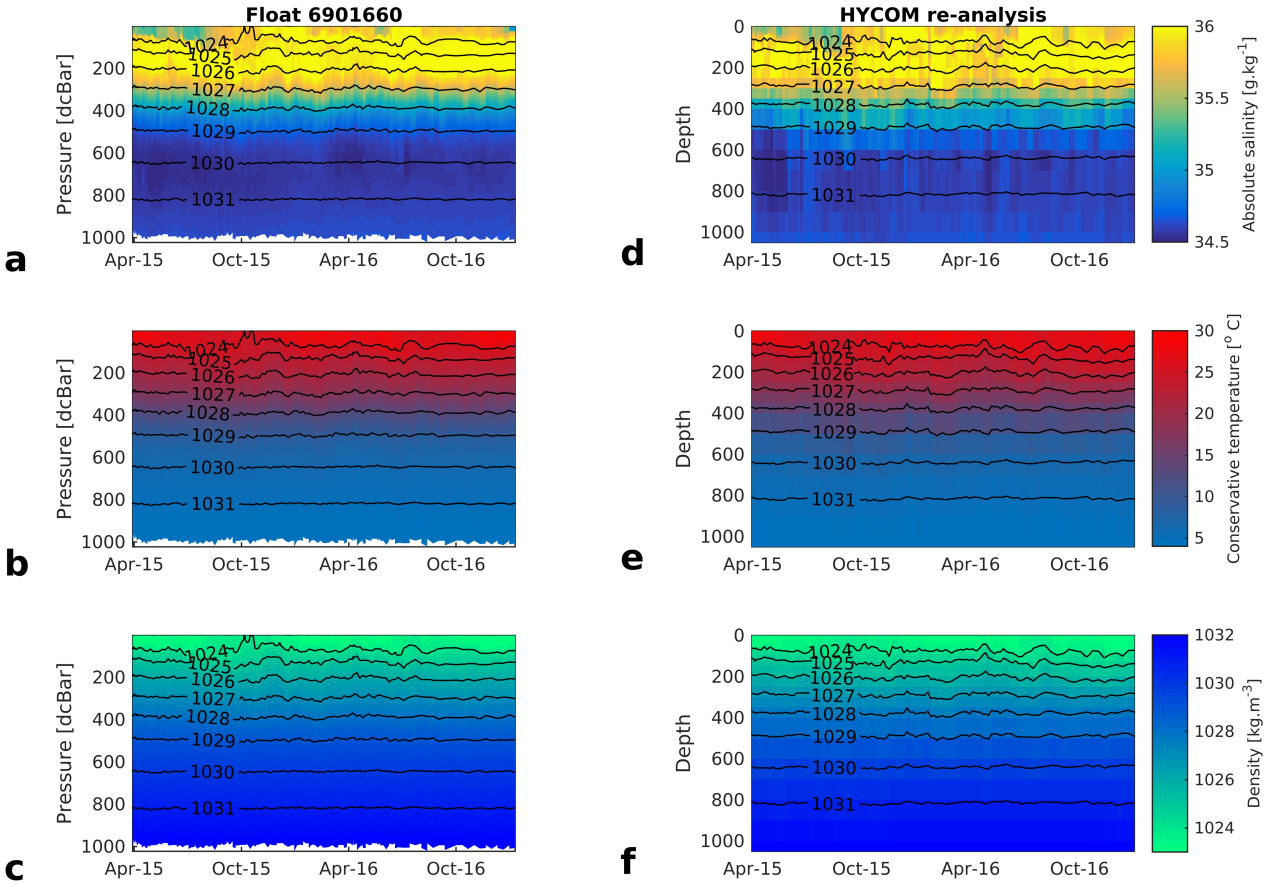

FIGURE C2 : Profiles of (left side) float 660 and (right side) corresponding data from HYCOM re-analysis over depth and time for (a,e) absolute salinity, (b,f) conservative temperature and (c,g) density. Every colored point corresponds to a measurement. The black lines indicate the isopycnals from 1024 to 1031 kg.m^{-3}.

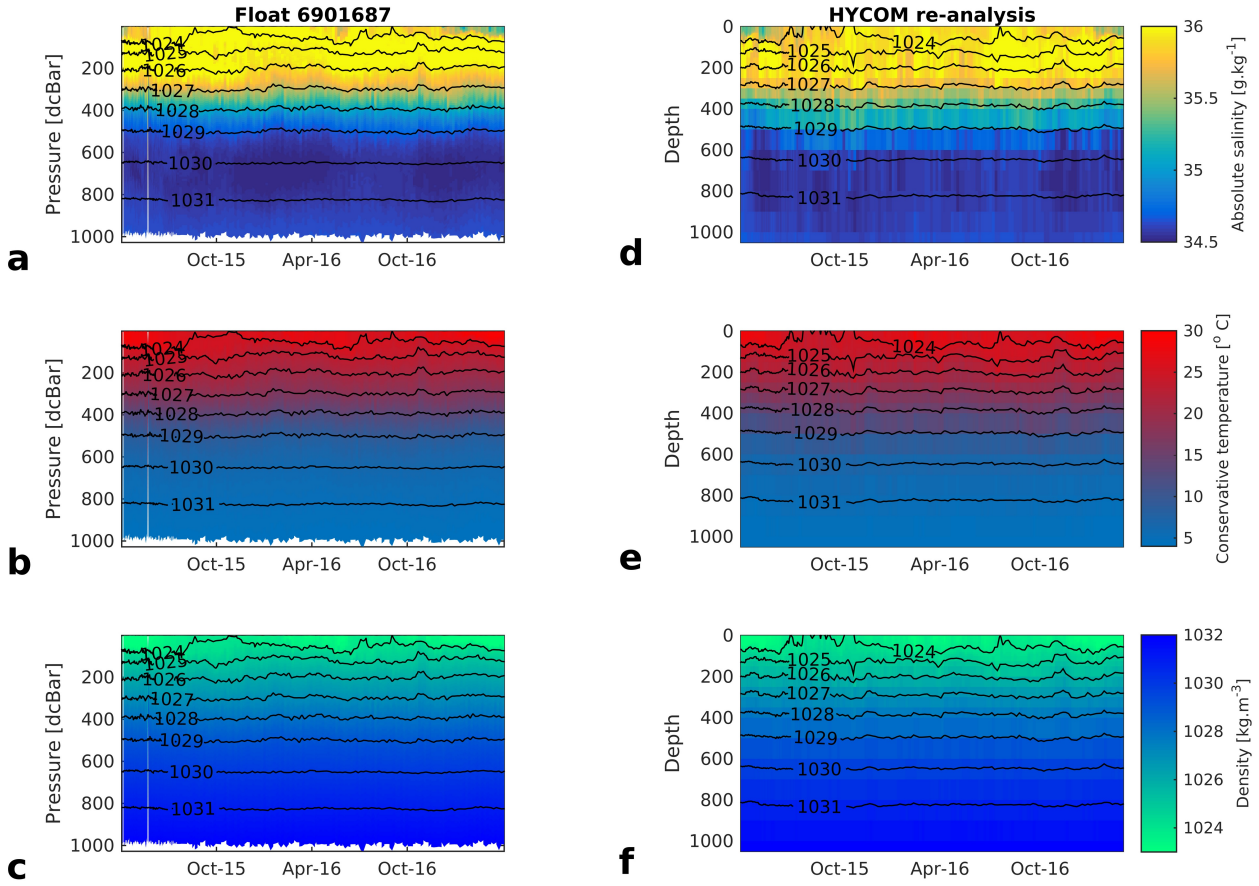

FIGURE C3 - Profiles of (left side) float 687 and (right side) corresponding data from HYCOM re-analysis over depth and time for (a,e) absolute salinity, (b,f) conservative temperature and (c,g) density. Every colored point corresponds to a measurement. The black lines indicate the isopycnals from 1024 to 1031 kg.m^{-3}.

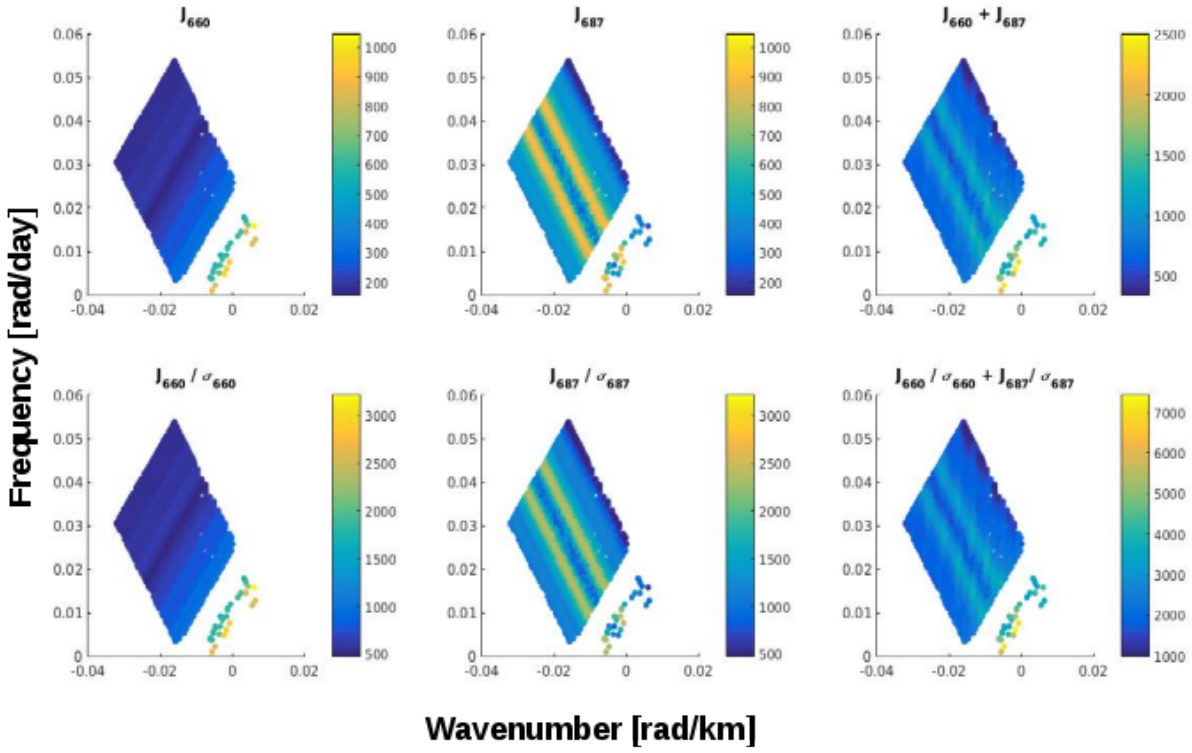

FIGURE J : Detail of J-index calculation for (left) the float 660, (center) the float 687 and (right) the overall J-index in a case without normalization (upper panels) and normalized with the standard deviation of the latitude of each float.

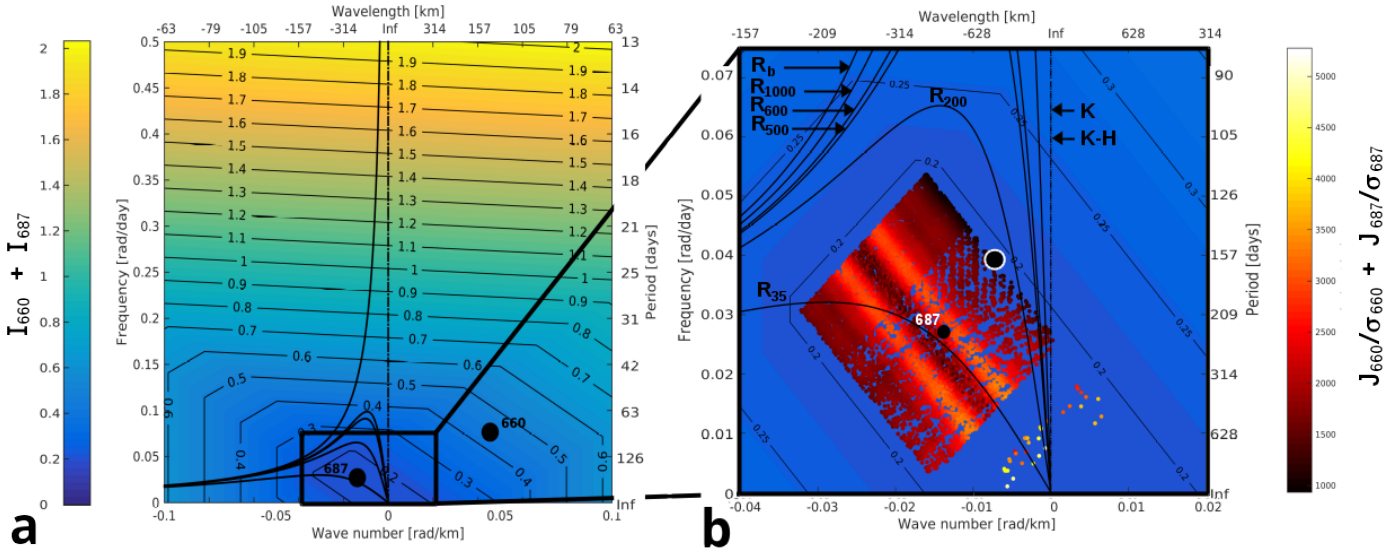

FIGURE 6 : Difference between observed Lagrangian float wave characteristics and Lagrangian theoretical wave ones (index **I**, left colorbar) for (a) the sum of floats 660 and 687 and (b) the associated minimum calculations (normalized index **J**, right colorbar) with regard to dispersion equations of Rossby wave (solid line), Kelvin wave (dotted line), Kevin-Helmholtz instability wave (break line). Subscript b means a barotropic case, subscripts with number means a baroclinic case with a stratification at the depth of this number. The negative wavelength describes a westward wave. Black dots indicate the observed Lagrangian parameters; note that on (b) only the 687 one is inside the range; the darker red dots show the minima of the index hence the best parameters that can explain both trajectories; the black surrounded by white dot is the couple (ω_{TMe} , k_{TMe}) that better fits the 660 and 687 float trajectories.

1200 m, around the AAIW. We can note the meridional gradient of salinity at the parking depth of the float, around 1000m"
Again, if HYCOM can be used, it would also be interesting to indicate whether the salinity, density and water mass gradient is indicated with the two floats. This important point has been raised previously and, please, refer to figures C2 and C3 above.
Otherwise, the earlier comment on the different striation in HYCOM compared to the observations raises some questions on where the fronts are located. Already answered; indeed we can not compare them directly like that.
p. 15, l. 25: 'It cannot be ruled out. . .' You could write more directly: 'It is likely that this eddy influenced the float trajectory. . .' Done
p. 15, l. 27: 'during the whole period' Done
p.17 and 18, first par. Of 4.1 Coral Sea. I am not completely sure on how different the two hypotheses are, and the way they are introduced could be clarified. The first one corresponds to a transport inside the core of a mesoscale structure (here C2) ; the second one to a transport on the edges of structures (here between C2 and A). We have substituted the sentence "Hence, we can also make a second...C2 to the west." by :
"Hence, we propose a second hypothesis of an edge transport for the NVJ waters going south. These waters could be first carried by the northern edge of A and then be transported southward thanks to the current located between A to the east and C2 to the west."
Again, how different/similar is HYCOM compared to the float data. Do we trust the position of the eddies in HYCOM, and if so to within which uncertainty? As explained above, HYCOM assimilates Argo float data. We do trust the position of C2 and A in HYCOM re-analysis because we also observe them in AVISO velocity maps. This is not the case for C1 which position differs between AVISO and HYCOM re-analysis. But again, to quantify the uncertainty of HYCOM re-analysis compared to observations would require a complete study and is beyond the scope of our study.
p. 18, l. 12: 'of turbulence' Done
p. 18, l. 15: replace 'could' by 'would'. Done
p. 18, l. 26: rewrite the sentence: 'We detail this sentence. . .' Done
p. 18, l. 31: 'the precision of the values. . .' I was indeed expecting a discussion on uncertainties on these values, when they were presented. Because of the complex shape of the J-index values (see above) we cannot give a precision like $\pm$ XX m-1. On the figure we can observe that the minima are 'organized' by lines, which is due to the conversion from Lagrangian wave couple characteristics to Eulerian ones. Indeed, many Eulerian couples could refer to a single Lagrangian couple if all the characteristics were variable. Unfortunately, we do not have any information on a potential Eulerian wave characteristic, especially at that depth (no mooring data in the region and period). As explained by Flierl (1981), "the Eulerian spectrum may contain only one frequency while floats set at different location will have different periods.". Thus, we constrained our problem using two floats with distinct Lagrangian wave characteristics to find a single Eulerian couple of characteristics.
p. 19, l. 14-15. I think that the sentence is not required. There is interest both in the average flow and in knowing that it is variable. Done
p. 20, l. 5: I am sure that this is not a 'new' proposed pathway, but I don't have a clear example on mind. We have changed the sentence "Moreover, the hypothesis...far as we know." by :
"Moreover, the hypothesis that the waters can be transported on the edge of several eddies is a new proposed pathway for NVJ waters."
p. 20, l. 10: 'recourse to' not used properly: not sure what is meant, but maybe 'biogechemical model simulations would help. . .' « resort to » should be better Done
p. 20, l. 13: 'water mass properties. . .' Done
p. 20, l. 16 'correction the impact of. . .' I am not sure what is corrected? We have changed the sentence "Correcting the impact...zonal directions." by :
"In order to convert Lagrangian wave observations to Eulerian ones in a simplified case, we concentrated on two floats, heading in opposite zonal directions. Moreover, we chose two PROVBIO floats in order to assure that their motions are representative of depth dynamics (as explained in Section 2.1)."
p. 20, l. 29: the sentence could be 'This study also underlined the importance of eddies in addition to the waves for the mesoscale dynamics of intermediate flows' Done

Interactive comment on “Intermediate water flows in the South West Pacific from OUTPACE and THOT Argo floats” by Simon Barbot et al.
Received and published: 23 April 2018

Response to : Anonymous Referee #2

This paper explores aspects of intermediate water flows in the southwest and central Pacific using individual Argo floats. From an analysis of low oxygen intrusions in a float flowing within the NCJ the authors argue that they originate from the NVJ–advected by cyclonic eddies. The variable oscillatory trajectories of zonally propagating floats are examined in detail. The Lagrangian and Eulerian characteristics are determined. Their analysis shows that a single Rossby wave can explain the trajectories of 2 floats travelling in opposite directions. A further section considers the salinity and density structure at 1000m (the Argo parking depth) and the impact on the float trajectories.

I find that the paper lacks any overall focus. It comes across as a few mildly interesting but unconnected observations. They all involve aspects of the circulation in the region but ultimately do not make a coherent story. The content is simply not strong enough to be suitable for publication.

Our manuscript contains two parts that have been found interesting by specialists of the Coral sea concerning the first part, and more generally by physical oceanographers concerning the wave impact at intermediate depth deduced from Argo trajectory for the second one. Moreover, they both have repercussions on biogeochemistry that are of interest to a more expanded community, and in particular to the OUTPACE community; hence the submission as one paper in this Special Issue. Another reason for gathering them in one manuscript is that both studies derive from focusing on float trajectories taken on individual basis; point that we propose to stress with the new title (see below).

Further Comments
The title is very specialized. How many readers would know the meaning of the OUTPACE and THOT acronyms? Another proposition is: "Intermediate water flows in the South West Pacific : contribution from individual Argo floats"
Page 1, Line 16 - ...(WTSP) interests is of interest to the biogechemical ... Done
Page 2, line 18 – Change to ’BGC data from the float allow us to determine whether it has encountered water masses coming from the NVJ. Done
2, line 35 - ...during the OUTPACE cruise or in the framework of the THOT project. Why are you canceling the signification of the THOT acronym and the reference to THOT ? "(TaHitian Ocean Time series, Martinez et al. 2015)"
4, line 1 – we also replace place the float trajectories .... Done here and everywhere else in the article.
4, line 10 - For memory, it begins with the descent of the float The float descends to a depth around 1000m, called ... We have modified the sentence accordingly : "This cycle starts with the descent of the float to a depth around 1000 m, called..."
4, line 25 – An error estimate should be provided. We have added the Table:

Table 1: Statistics for the different floats between surface and deep trajectories, the results are presented as ’mean $\pm$ std’.

Float	Type	Surface distance [km]	Deep distance [km]	Surface speed [cm/s]	Deep speed [cm/s]
656	PROVBIO	0.44 ± 0.23	17.32 ± 18.18	29.57 ± 15.83	4.30 ± 3.93
660	PROVBIO	0.35 ± 0.18	15.96 ± 9.28	25.77 ± 13.16	3.65 ± 1.87
671	ARVOR	6.08 ± 3.44	25.30 ± 14.04	28.37 ± 16.12	3.00 ± 1.67
679	ARVOR	4.84 ± 2.38	21.88 ± 12.17	22.44 ± 11.07	2.60 ± 1.45
687	PROVBIO	0.33 ± 0.19	8.54 ± 6.53	24.26 ± 13.20	3.66 ± 1.89

To satisfy both you and the other reviewer, we have also replaced the sentence "After some verifications...deep displacement." by the paragraph :

"Table 1 shows the mean properties of each studied float. First, it highlights the differences in surface distances between PROVBIO and ARVOR floats. At the surface, ARVOR floats drift over a distance about 10 times greater than PROVBIO floats. This is due to the longer time they spent at the surface (6h for ARVOR floats and 24min for PROVBIO one). The ratio between deep and surface distances is a factor of 30 for PROVBIO floats and still 4 for ARVOR ones. Float 656 exhibits anomalously high standard deviation for its deep distance and deep speed. These high values, equal to the mean ones, are due to the period during which the float was grounded on the sea floor in the Queensland plateau. Otherwise we have concluded that surface displacements can be neglected compared to deep displacements without doubt for PROVBIO floats and with caution for ARVOR floats. Hence, when needed in the wave section, we will only use the former ones and consider that the trajectory dynamics are mainly due to deep circulation processes. The discussion of such considerations is thoroughly made by Ollitrault and Rannou (2013)."

5, line 3 – Trajectory description for the a wave approach We have changed it to : "Wave characteristics from float trajectory"

5, line 4 – What type of waves? We have modified the first sentence of this section to make it more explicit: "Here the objective is to find the characteristics of a single wave that could explain the float trajectories which represent both retrograde and prograde circulation (retrograde when Lagrangian motion is in the opposite direction as the wave propagation; prograde when Lagrangian motion and wave propagation are in the same direction; as defined in Flierl, 1981)".

11, line 14 – we could hypothesized hypothesize that such ... Done

15, line 2 - ...we are able to replace place the trajectory... Done

15, line 6 – This appears to be stating the very obvious point about the two different velocity observations. Sentence removed

18, 4 - ..and then be transported southwards thanks to by the current located... Done

18, line 7 - ..widen the comprehension understanding of the connection ... Done

18, line 7 – and the NCJ and claim for the suggest that there be an explicit consideration of mesoscale eddies eddy variability in future modeling approach approaches. Done

20, line 8 – .... To replace place the Done

20, line 13 – of water masses properties, Done

20, line 16 – form a favorable context environment... Done

20, line 16 – Not sure what you mean by the sentence beginning 'Correcting the impact of the Lagrangian observation We have changed the sentence "Correcting the impact...zonal directions." by :

"In order to convert Lagrangian wave observations into Eulerian ones in a simplified case, we concentrated on two floats, heading in opposite zonal directions, and hence providing both cases of prograde and retrograde motions."

20, line 20 – would require to wait until the time series are longer a longer time series. Done

A large portion of the paper (1/3) deals with the methods and description of decomposing the float trajectory into a wave framework. A briefer description of the method would be more appropriate for the paper. We agree that the method section is a bit large but, since this article is proposed for publication in the OUTPACE Special Issue mainly composed of biogeochemistry articles, we made the choice to start the explanation of the methods with a very generic/basic framework, accessible to all oceanographers and not only physical oceanographers.

The figure generally are poor, the captions are tiny and difficult to read. Figure 9 is simply impossible to distinguish any of the contours. To summarize the figures are below the standard required for publication. Any submission for review should provide figures that are ready for publication., all the figure were reprocess to get a decent resolution Done. We have reprocessed all the figures and set them with an adequate resolution to avoid any inconvenient or misreading. The revised version can be transmitted as soon as requested.

Intermediate water flows in the South West Pacific ~~from OUTPACE and THOT~~ : as revealed by individual Argo floats trajectories and a model re-analysis

Simon Barbot[1], Anne Petrenko[1], and Christophe Maes[2]

[1]Aix Marseille Université , CNRS/INSU, IRD, Université du Sud Toulon-Var, Mediterranean Institute of Oceanography (MIO), UM 110, 13288 Marseille

[2]Laboratoire d'Océanographie Physique et Spatiale (LOPS), CNRS, Ifremer, IRD, UBO, Brest, France

Correspondence to: Simon Barbot (simon.barbot@legos.obs-mip.fr)

Abstract. Thanks to the autonomous Argo floats of the OUTPACE cruise and of the THOT project, some features of intermediate flow dynamics, around 1000 m depth, within the Southwest and Central Pacific Ocean (156^{o}E-150^{o}W, around 19^{o}S) are described. In the Coral sea, we highlight minima in dissolved oxygen of 140 μmol.kg^{-1} that are associated with the signature of a southward transport of waters between two zonal jets: from the North Vanuatu Jet to the North Caledonia Jet. This transport takes place in the core of a cyclonic eddy or via the path between a cyclonic eddy and an anticyclonic one, highlighting the importance of mesoscale dynamics in upper thermocline and surface layers. Further east, we observe a strong meridional velocity shear with long-term float trajectories going either eastward or westward in the lower thermocline. More interestingly, these trajectories also exhibit some oscillatory features. Those trajectories can be explained by a single Rossby wave of 160 days period and 855 km wavelength. Considering the thermohaline context, we confirm the meridional shear of zonal velocity and highlight a permanent density front that corresponds to the interface between Antarctic Intermediate Waters and North Pacific Deep Waters. Hence both circulation and thermohaline contexts are highly favorable to instabilities and wave propagation.

1 Introduction

The intermediate water masses have been known to be of great importance for the thermohaline overturning circulation (Las Heras and Schlitzer, 1999) and for biogeochemical cycles (Ganachaud and Wunsch, 2002) all over the oceans. More specifically, the Western Tropical South Pacific (WTSP) ~~interests~~ is of interest to the biogeochemistry community because of its oligotrophic and ultra-oligotrophic zones where diazotrophy has a large influence on phytoplankton growth (Bonnet et al., 2017; Benavides et al., 2017; Caffin et al., 2017). To make progress on this subject, the OUTPACE cruise (Oligotrophy to UlTra-oligotrophy PACific Experiment ; Moutin et al., 2017), on board the R/V L'Atalante, took place during spring 2015. The surface circulation of the cruise context has been studied in order to understand the impact of meso- and submeso-scale on an observed bloom (de Verneil et al., 2017b), on the horizontal distribution of biogeochemical/biological components (Rousselet et al., 2017) and ~~re~~placing them in the large-scale circulation of the Western Tropical South Pacific (Fumenia et al., 2018).

Our study will ~~complete~~ complement these observations of the surface circulation both in space, by focusing on intermediate levels, and in time, by using the time series (more than two years) of the autonomous Argo floats deployed during the cruise.

~~Autonomous Argo floats are useful to study intermediate circulation and biogeochemistry and biology of the first thousand meters of the water column, when they are also BGC floats. Such approaches lead to~~ Autonomous Argo floats are profilers parked at 1000 m depth and reaching the surface every 10 days, where they transmit their measurements and location (further information on the cycle of the different Argo floats we used is detailed in the next section). Current speeds at the parking depth of the floats are then calculated, leading to horizontal gridded maps of velocities either global (Davis, 2005; Ollitrault and Rannou, 2013) or regional (Cravatte et al., 2012). Other approaches are developed in order to study the intermediate circulation, for example, by taking into account the spreading of different float trajectories from a same position (Sevellec et al., 2017). Moreover, when Argo floats are BCG, on top of allowing the study of intermediate circulation, they provide measurements of biogeochemistry and biology parameters over the first thousand meters of the water column.

In a sense, the studies focusing on the specificity of one particular trajectory (e.i. Mitchell, 2003; Boss et al., 2008; IOCCG, 2009; Bishop and Wood, 2009; Phillips and Bindoff, 2014) are less frequent now that data from many floats have become available. Our approach focuses on a few float trajectories using them as witnesses of intermediate waters specific dynamics.

The cruise started in the Coral Sea, where the main upper currents are characterized by narrow jets named the North Vanuatu Jet (NVJ) and the North Caledonia Jet (NCJ) at the entrance of the Coral Sea. Both of them are westward zonal jets (Fig. 1a, Webb, 2000) but the water masses they carry at the level of the main thermocline are not identical. Gasparin et al. (2014) examine the composition of water masses and report a net difference in dissolved oxygen concentration (DOXY) with waters ~~more deoxygenated~~less oxygenated in the NVJ than in the NCJ. These two jets derive from different branches of the South Equatorial Current (SEC), a broad current with prevailing geostrophic westward currents (Fig. 1a). ~~The NVJ originates from a longer branch, hence its lower DOXY.~~ The NVJ is older, in the sense that it originates from a longer path than the NCJ, since its last contact to the surface. Hence, without ventilation, the DOXY of the NVJ intermediate waters is lower than the NCJ DOXY. Using DOXY as a proxy to make the difference between NVJ and NCJ, Rousselet et al. (2016) revealed an intrusion of NVJ waters in the NCJ pathway during the BIFURCATION cruise (Maes, 2012). The former authors concluded that the NVJ waters were transported southwards by a mesoscale anticyclonic eddy. Here the BGC Argo float deployed at the Long Duration station A (LDA) of OUTPACE, north of New Caledonia, has followed the path of the NCJ.~~Its BGC data allow to test whether, during its path,~~Changes in the float BGC data allow us to determine whether it has encountered water masses coming from the NVJ.

Further east, other Argo floats, deployed during OUTPACE, are characterized by a main eastward displacement in opposite direction compared to the westward SEC (Fig. 1a). Observations in other regions of the world revealed a complex alternation of zonal currents, now known as striations, in surface zonal velocity estimated with altimetric products (e.g. Maximenko et al., 2005, 2008). These striations have also been found, more recently, at intermediate levels with Argo floats (Fig. 1c, Cravatte et al., 2012; Ollitrault and Colin de Verdière, 2014). More detailed works are underway on such striations in order to observe them more precisely and to understand their physics (Cravatte et al., 2017; Belmadani et al., 2017). During the OUTPACE cruise, Rousselet et al. (2017) highlighted the velocity anomaly of such striations at the surface in one specific area close to

the OUTPACE domain (160^{o}E-150^{o}W and 18^{o}S-22^{o}S). Thanks to the floats we can extend this observation at intermediate levels and several years after the cruise. In our case, two intermediate water masses are present near the parking depth of the floats, around 1000 m: the Antarctic Intermediate Waters (AAIW) to the south and the North Pacific Deep Water (NPDW) to the north (Fig. 1b).

The first part of this study focuses on the mesoscale interactions between NCJ and NVJ within the Coral Sea. Thanks to Argo float WMO6901656, equipped with an optode sensor, we analyze the DOXY variability over the 2015-2016 period using it as a proxy in order to distinguish NCJ waters from NVJ ones. Then, we ~~re~~place the DOXY anomalies in their thermohaline and circulation context. In a second part, we focus on the central Pacific Ocean zone where we describe specific trajectories of floats deployed during the OUTPACE cruise or in the framework of the THOT project (TaHitian Ocean Time series, Martinez et al., 2015). Once again, we also ~~re~~place the float trajectories in their thermohaline and circulation context. In order to explain their displacement at mid-depths we choose a wave approach and compare our results, taking into account Doppler shift, to different cases of Rossby, Kelvin and Kelvin-Helmholtz instability waves. Then, we discuss the proposed hypothesis for the two areas and what they imply for the OUTPACE observations. Finally, we conclude and propose some method improvements.

2 Data sets and methodology

2.1 Autonomous floats

In the present study we benefit from the deployment during the 2015 spring of several Argo floats (http://doi.org/10.17882/42182) under the auspices of the OUTPACE cruise (Moutin et al., 2017) and of the THOT project (Martinez et al., 2015). We analyze the two first years of data. All OUTPACE and THOT floats are related to the Argo international program and have the same type of sampling cycle. ~~For memory, it begins~~ This cycle starts with the descent of the float to a depth around 1000 m, called the parking depth where the floats drift for a programmed time. This time can be remotely modified in the last generation of floats, ~~like~~ such as those used in this study. Here we use the measurements made while the floats rise to the surface. At the surface, these data are transmitted via satellite. Even if this cycle is the same for all floats, the time spent at the parking depth (in our cases, 5 or 10 days), and hence the corresponding sampling frequency (Δt), are not the same for all of them. Two types of float are available: ARVOR (Argo-Core) floats and PROVBIO floats (Bio-Argo). Because they were all ~~immersed~~ deployed during the same months, they all have a close WMO code : #6901XXX. Hereafter, ~~to ease the writing of the float number,~~ we only use the three last digits of the float number to ~~point~~ refer to them, i.e. float 656 refers to #6901656. In this study, we use three PROVBIO floats using Iridium (656, 660 and 687) and two ARVOR floats using ARGOS (671 and 679). Details and data are accessible via the CORIOLIS operational center (www.coriolis.eu.org). In order to get the average velocity of the floats during their cycles, we follow the method of Ollitrault and Rannou (2013) taking different time slots over the float cycle in order to calculate, for the n$^{\text{th}}$ cycle, the surface velocity $V^n(0)$ and the velocity at 1000 m $V^n(1000)$:

$$V^n(0) = \frac{L^n_{\text{last}} - L^n_{\text{first}}}{t^n_{\text{last}} - t^n_{\text{first}}}, \qquad V^n(1000) = \frac{L^n_{\text{first}} - L^{n-1}_{\text{last}}}{t^n_{\text{first}} - t^{n-1}_{\text{last}}} \tag{1}$$

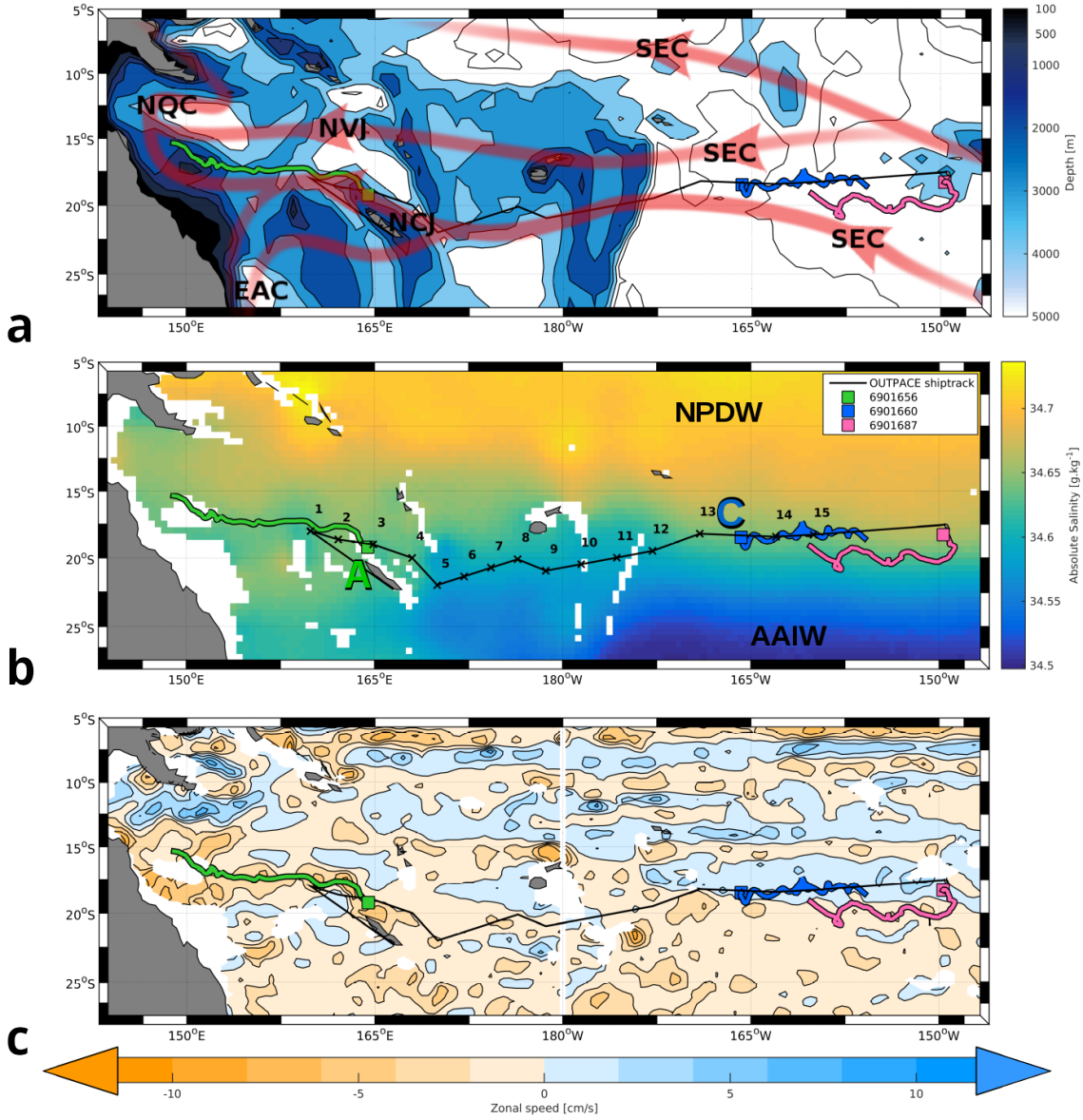

Figure 1. South-west Pacific Ocean (a) main trajectories of zonal jets superimposed on the bottom topography (in m), (b) absolute salinity (g.kg^{-1}) at 1000 m for November climatology from the ISAS13 atlas and (c) zonal mean current (in cm/s, positive for eastward velocity) deduced from the Argo float displacement at their parking depth (near 1000 m, adapted from Ollitrault and Colin de Verdière, 2014). The colored lines represent the studied floats (WMO number in the inset) with squares for their immersion location. The currents shown in the upper panel are the South Equatorial Current (SEC), the North Vanuatu Jet (NVJ), the North Caledonia Jet (NCJ), the North Queensland Current (NQC) and the East Australia Current (EAC). The water masses shown on the middle panel are the North Pacific Deep Water (NPDW) and the Antarctic Intermediate Waters (AAIW). The black line represents the shiptrack of the OUTPACE cruise and, in the middle panel, the crosses represent the short time stations (numbers) and the squares A and C represent two the long time stations of the cruise where the ~~studied~~ floats in this study were deployed.

where L_{first} and L_{last} are the first and the last transmitted location in the same cycle ~~(PROVBIO floats transmit only two locations per cycle using Iridium whereas ARVOR floats transmit seven locations per cycle using ARGOS)~~ and t is the corresponding time. ~~After some verifications we have concluded that, even if the mean surface velocity is ten times greater than the mean deep velocity, each float stays such a short time at the surface that its displacement there can be neglected compared to the deep displacement.~~

Table 1. Statistics for the different floats between surface and deep trajectories, the results are presented as 'mean $\pm$ std'.

Float	Type	Surface distance [km]	Deep distance [km]	Surface speed [cm/s]	Deep speed [cm/s]
656	PROVBIO	0.44 ± 0.23	17.32 ± 18.18	29.57 ± 15.83	4.30 ± 3.93
660	PROVBIO	0.35 ± 0.18	15.96 ± 9.28	25.77 ± 13.16	3.65 ± 1.87
671	ARVOR	6.08 ± 3.44	25.30 ± 14.04	28.37 ± 16.12	3.00 ± 1.67
679	ARVOR	4.84 ± 2.38	21.88 ± 12.17	22.44 ± 11.07	2.60 ± 1.45
687	PROVBIO	0.33 ± 0.19	8.54 ± 6.53	24.26 ± 13.20	3.66 ± 1.89

Table 1 shows the mean properties of displacements for each studied float. First, it highlights the differences in surface distances between PROVBIO and ARVOR floats. At the surface, ARVOR floats drift over a distance about 10 times greater than PROVBIO floats. This is due to the longer time they spent at the surface (6h for ARVOR floats and 24min for PROVBIOs). The ratio between deep and surface distances is a factor of 30 for PROVBIO floats and still 4 for ARVOR ones. Float 656 exhibits anomalously high standard deviation for its deep distance and deep speed. These high values, of the same order as the mean ones, are due to the period during which the float was grounded on the sea floor in the Queensland plateau. Otherwise we have concluded that surface displacement can be neglected compared to the deep displacement without doubt for PROVBIO floats and with caution for ARVOR floats. Hence~~we can~~ , when needed in the wave section, we will only use the former ones and consider that the trajectory dynamics are mainly due to deep circulation processes. The discussion of such consideration is thoroughly made by Ollitrault and Rannou (2013).

In the case of the 656 float, we also consider the dissolved oxygen concentration (DOXY) measurements. These data were calibrated (A. Fumenia, personal communication) based on the CTD profiles made just before the float was ~~immersed~~ deployed during the OUTPACE cruise. The calibration for the 656 float is:

$$DOXY_{\text{clb}} = 0.97125\, DOXY_{\text{raw}} + 14.3755 \tag{2}$$

where $DOXY_{\text{raw}}$ is the dissolved oxygen concentration data from the float and $DOXY_{\text{clb}}$ is the calibrated dissolved oxygen concentration data, both expressed in μmol.kg^{-1} .

2.2 ~~Trajectory description for the a wave approach~~ Wave characteristics from float trajectories

~~Here the objective is to explain the float trajectories influenced by waves.~~ Here the objective is to find the characteristics of a single wave that could explain the float trajectories which represent both retrograde and prograde circulation (retrograde

when Lagrangian motion is in the opposite direction as the wave propagation ; prograde when Lagrangian motion and wave propagation are in the same direction; as defined in Flierl, 1981).

Thus, we describe the float trajectories as Lagrangian description of waves, using the period T and the wavelength λ as well as the frequency ω ($\omega = 2\pi/T$) and the wavenumber k ($k = 2\pi/\lambda$). ~~The wavenumber is defined as:~~

$$k^2 = k_v^2 + k_H^2 = k_v^2 + k_{lon}^2 + k_{lat}^2 \tag{3}$$

~~where k_v is the vertical wavenumber, k_H the horizontal one, k_{lon} the longitudinal one and k_{lat} the latitudinal one.~~ In our case, the dynamics of the floats do not allow us to raise information concerning the vertical component because data on float locations are only measured at the surface. The displacements of the floats are mostly directed by the currents, and only secondarily by waves. Since the prevailing currents are mainly zonal, we consider hereafter, to simplify, that the wavenumbers derived from the observations correspond to the longitudinal component ($k = k_{lon}$). To clarify the methodology, we choose to name "float wave" the measured wavy trajectory of a float and "theoretical wave" the process that could lead to such trajectory.

We tried to describe the float waves with a Fourier transform or a wavelet analysis on the float time series, but the description of the different frequencies contained in them was incomplete. This is due to the shortness of the time series (2 years) with regard to the sampling period. If the floats are still functional in a few years, these methods should be reconsidered.

So instead, we developed the method presented here, with Lagrangian and Eulerian wave descriptions and the estimations of wavenumbers. In order to maximize the information derived from the portions of the trajectories where the floats oscillate, we choose ~~to determine half float wave characteristics rather than full float wave ones~~ not to describe the complete float wave characteristics (T, λ) but their halves ($T/2$, $\lambda/2$). In practice, this means we measure time and distance from crest to trough (and so on) rather than from crest to crest, for each ~~float~~ studied float (floats 660, 671, 679 and 687, Fig.2). ~~Hence, we obtain a double number of more precise measurements of $\lambda/2$ from the position maps, and of $T/2$ from the float time series of latitude.~~ Hence, it allows to have more estimates when incomplete cycles are present. The measurements of $\lambda/2$ are made from the position maps and of $T/2$ from the float time series of latitude.

Because the floats are, by definition, Lagrangian devices, we need to be careful before comparing the float waves to the classical Eulerian oceanic waves. We first use a simple case to get a basic relation between Eulerian wave parameters and Lagrangian ones. Because of the zonal tendency of the studied float trajectories (Fig. 2), we express a simple case of the current perturbations due to a homogeneous, monochromatic wave (hereafter plane wave) propagation with the following system of equations :

$$\begin{cases} u = u_0 \\ v = v_0 \sin\left(\omega_{Te} t - k_{Te} x + \varphi_{Te}\right) \end{cases} \tag{4}$$

where u_0 and v_0 are zonal and meridional velocities considered as constants, ω_{Te} is the frequency, k_{Te} is the wavenumber and φ_{Te} is the phase shift term of the Eulerian theoretical wave. Note that v_0 is the amplitude A_{Te} of the Eulerian theoretical wave. By convention, the subscript 'T' is used for theoretical, 'M' for measured, 'e' for the Eulerian description of the wave and 'ℓ' for the Lagrangian one (Tab. 2). After performing some tests (Appendix A), we choose to set the zonal velocity of the floats as

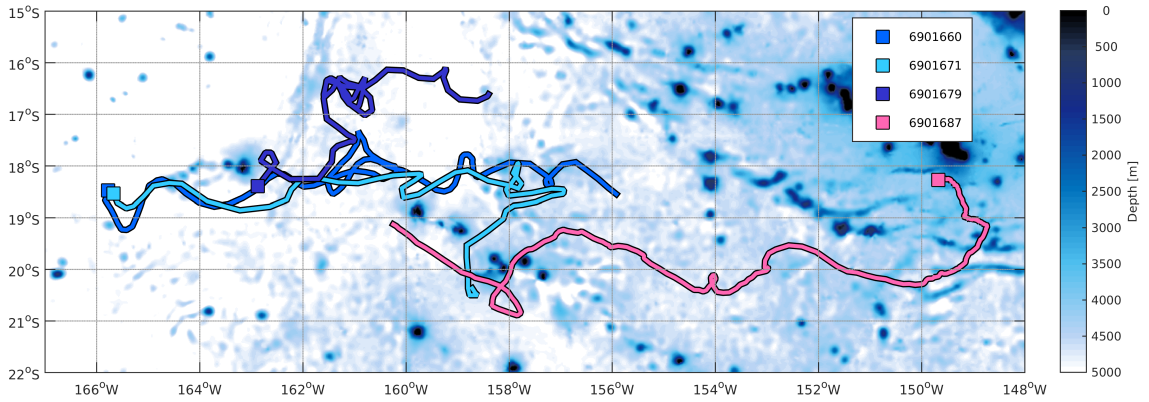

Figure 2. Trajectories of the studied floats superimposed on bottom topography (in m). The squares represent the initial location of the floats.

the global mean velocity of the float trajectory:

$$u_0 = \begin{cases} \frac{L^{\text{end}} - L^1}{t^{\text{end}} - t^1} = 1.65 \text{ cm/s} & \text{for float 660} \\ \\ \frac{L^{\text{end}} - L^{58}}{t^{\text{end}} - t^{58}} = -1.93 \text{ cm/s} & \text{for float 687} \end{cases} \tag{5}$$

where L^{end} is the location of the float at the last cycle. For float 687, the 58th cycle corresponds to the start of the float westward propagation. Thus, we only consider the 687 float trajectory from the 58th cycle to the end location.

In such a configuration, the Lagrangian observation of the float can be represented by a Doppler effect on the perception of the theorical wave. So we can express the Lagrangian properties of the theoretical wave ($\omega_{\text{T}\ell}$, $k_{\text{T}\ell}$ and $A_{\text{T}\ell}$) as a function of ω_{Te}, k_{Te}, A_{Te} and u_0:

$$\begin{cases} \omega_{\text{T}\ell} = \omega_{\text{Te}} - k_{\text{Te}} u_0 \\ k_{\text{T}\ell} = k_{\text{Te}} - \frac{\omega_{\text{Te}}}{u_0} \\ A_{\text{T}\ell} = -\frac{A_{\text{Te}}}{\omega_{\text{Te}} - k_{\text{Te}} u_0} \end{cases} \tag{6}$$

But these equations derive from one common expression, hence this system cannot be solved like a 3 equations - 3 unknowns one. Solving 6 is then not trivial without setting either ω_{Te} or k_{Te}. So we need another method to find the Eulerian properties of

Table 2. Summary of the different notations of the wave properties : frequency ω, wavenumber k and amplitude A.

$\omega_{\text{M}\ell}$, $k_{\text{M}\ell}$, $A_{\text{M}\ell}$	Measured float wave, Lagrangian description.
$\omega_{\text{T}\ell}$, $k_{\text{T}\ell}$, $A_{\text{T}\ell}$	Theoretical wave, Lagrangian description.
ω_{Te} , k_{Te} , A_{Te}	Theoretical wave, Eulerian description.
ω_{TMe} , k_{TMe} , A_{TMe}	Theoretical wave that better fits the measured float waves, Eulerian description.

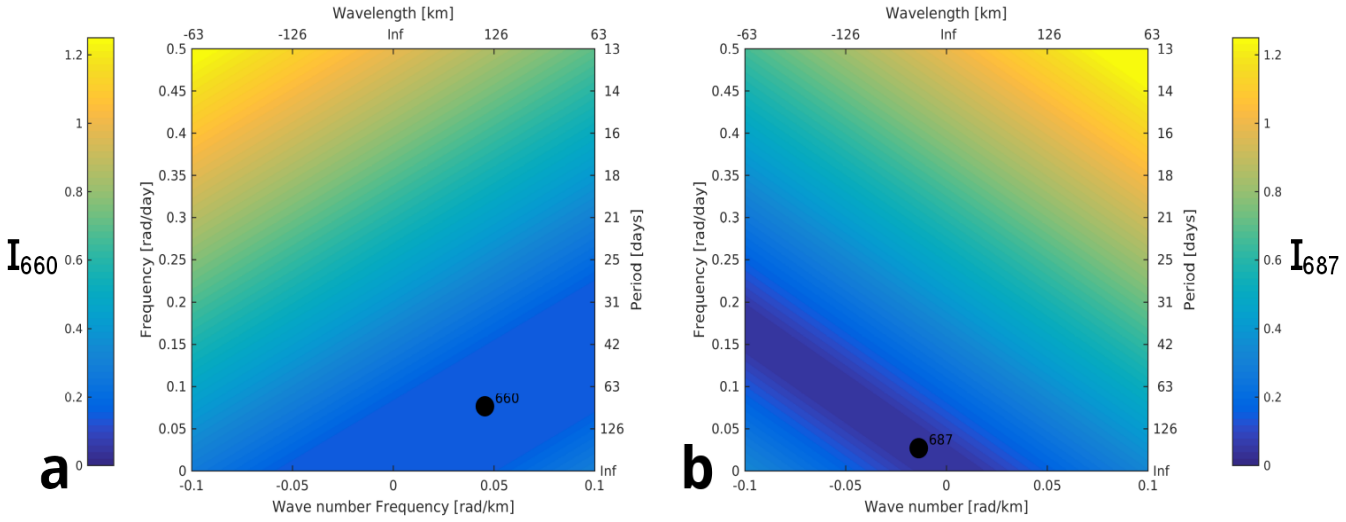

Figure 3. Difference between observed Lagrangian float wave parameters and Lagrangian theoretical wave ones (index **I**) for (a) float 660, (b) float 687. Negative wavelengths describe westward waves. Black dots indicate the observed Lagrangian parameters.

the theoretical wave that better fits the float trajectories. Hereafter, we use those equations in order to build an index I for the differences between the Lagrangian properties of the float waves ($\omega_{\mathrm{M}\ell}$ and $k_{\mathrm{M}\ell}$) and the Lagrangian properties of the potential theoretical waves ($\omega_{\mathrm{T}\ell}$ and $k_{\mathrm{T}\ell}$). I is defined by the following expression:

$$I_a = \left\{ \left| \omega_{\mathrm{M}\ell} - \omega_{\mathrm{T}\ell} \right| + \left| u_0 \left(k_{\mathrm{M}\ell} - k_{\mathrm{T}\ell} \right) \right| \right\}_a \tag{7}$$

where a is the float considered.

We made the calculations for a range of Eulerian frequencies and wavenumbers (ω_{Te} and k_{Te}), thanks to Equations 6, in order to get the diagrams of this index for float 660 (I_{660}, Fig. 3a) and for float 687 (I_{687}, Fig. 3b). For each index, the zone gathering all the index minima has a linear shape : positive for float 660 and negative for float 687. Hence, since these linear slopes are of opposite signs, minimizing the sum of the two ~~indexes~~ indices leads to find where the two lines of minima cross each over. The crossing approach determines the properties of the theoretical wave that could better fit both the float trajectories. This method could be used with several other floats and be expressed by the following formulation:

$$I = \sum_{na=1}^{N} I_{na} \tag{8}$$

where N is the total number of floats considered, in our study $N = 2$. Using this numerical approch, we can find all the couples (ω_{Te} , k_{Te}) that minimize I, and hence that could fit the float trajectories.

In order to compare the couples that minimize I and find the one that better fits the 660 and 687 float trajectories, we make a simulation of the idealized trajectory for each couple. The simulations use Equations 4, integrating them to express the

longitude $x(t)$ and the latitude $y(t)$ of Lagrangian particles as a function of time:

$$\begin{cases} x(t) = x_0 + u_0 t \\ y(t) = y_0 + \frac{v_0}{\omega_{\text{Te}} - k_{\text{Te}} u_0} \left[cos\left(\left(\frac{\omega_{\text{Te}}}{u_0} - k_{\text{Te}} \right) x(t) - \frac{w_{\text{Te}}}{u_0} x_0 + \varphi_{\text{Te}} \right) - cos\left(-k_{\text{Te}} x_0 + \varphi_{\text{Te}} \right) \right] \end{cases} \tag{9}$$

where x_0 and y_0 define the initial position of the float. The simulations run with a time step of 1 day for 642 days ($\left\{t^{\text{end}} - t^1\right\}_{660} = \left\{t^{\text{end}} - t^{58}\right\}_{687} = 642$ days in Equations 5). In order to compare the simulations to the float trajectories, we interpolate the latitudes of the float, y_{int}, at the longitudes of the corresponding simulations. Then we calculate the sum of the differences of latitude using an index J, defined as:

$$J_a = \left\{ \sum_{j=1}^{m} \mid y_{\text{int}}(j) - y_{\text{simu}}(j) \mid \right\}_a \tag{10}$$

where a is the considered float, y_{simu} are the latitudes of the simulation and m is the total number of days, here $m = 642$. Because the value of φ_{Te} can influence the value of J, we made several simulations for each couple (ω_{Te} , k_{Te}) varying φ_{Te} from $-\pi$ to π with a step of $\frac{1}{10}\pi$. As for index I, we can sum J_{660} and J_{687} to get the couple that minimizes the trajectory differences of both floats 660 and 687. Because the initial time of the two floats is the same, φ_{Te} must be the same for the two floats. Then we sum J_{660} and J_{687} for each φ_{Te}. This method could also be used with several other floats and be expressed by the following equation:

$$J = \sum_{na=1}^{N} \frac{J_{na}}{\sigma_{na}} \tag{11}$$

with σ the standard deviation of the latitude of the float.

These two steps give us the couple (ω_{TMe} , k_{TMe}) of the theoretical wave that better fits the trajectories of floats 660 and 687. This couple can now be compared to classical Eulerian oceanic waves such as Kelvin, Rossby and Kelvin-Helmholtz instability waves.

According to Flierl (1981), for each float, we can define

$$\varepsilon = \frac{u_0}{c} \tag{12}$$

where c is the phase speed of the wave ($c = \frac{\omega}{k}$). The sign of ε indicates the type of motion of the float (prograde or retrograde) and its amplitude compares the particle velocity to the wave speed.

2.3 Ancillary data

In order to evaluate the possible link between oxygen anomalies and surface currents in the Coral Sea, we use the AVISO altimetry products (www.aviso.altimetry.fr). We select ocean-level elevation anomaly products, reworked from all satellites, to obtain geostrophic velocity anomaly fields (u_g and v_g) with a 1/4 degree resolution. From those data we calculate the

geostrophic velocity amplitude. We also use HYCOM (HYbrid Coordinate Ocean Model) re-analysis GLBu0.08 of the experience 91.1 from March 2015 to March 2016 (www.hycom.org). This system is a hybrid isopycnal-sigma-pressure (generalized) coordinate ocean model with 1/12 degree horizontal resolution and 40 vertical levels, assimilating in situ data.

In order to ~~re~~place our analyses within the global thermohaline context, we used the ISAS13 atlas (In Situ Analysis System, Gaillard, 2012) that provides a climatology of thermohaline properties. This atlas collects and processes all the profiles provided by the Argo floats from 2004 to 2012 in order to calculate a monthly global climatology over the entire depth of the oceans. More details are provided by Gaillard et al. (2016). We apply the same methods to calculate the density as those used for HYCOM re-analysis.

In the following, whatever is the source for the temperature and salinity fields, the density of the water masses is computed with the Matlab toolbox Gibbs-Seawater based on the TEOS-10 convention (www.teos-10.org/software.htm).

3 Results

3.1 Coral sea

The trajectory of float 656 can be clearly associated with the flow along the New Caledonian coasts at the entrance of the Coral Sea (Gasparin et al., 2011, Fig. 1a). The float then travels westward until the Queensland plateau where it often reaches the bottom before stabilizing near its parking depth. Hence, from November 2015 to October 2016, it either moves very slowly or stays stuck in the same region. Afterwards the float moves northwestward circumventing the plateau at the end of the period analyzed here. This trajectory corresponds very strongly with the NCJ pathway. ~~Here we focus on the measurements made by this float.~~

3.1.1 The DOXY variability of the jets

The correspondence between Argo profiles and HYCOM re-analysis for conservative temperature, absolute salinity and density can be found in the Appendix C. As expected from a re-analysis that assimilates different measurements including Argo float data, the salinity and temperature are in good agreement with the float measurements.

In addition to the standard parameters of conservative temperature and absolute salinity, float 656 provides DOXY profiles. We plot the temporal evolutions of these properties, corresponding to a mainly East to West transect (Fig. 4). Whereas temperature and salinity vary quite homogeneously below the upper layers, we can observe a strong oxygen stratification of the water column: higher concentrations at the surface (around 200 μmol.kg^{-1}) and between 500 m and 900 m (around 190 μmol.kg^{-1}) and lower concentrations between 100 m and 500 m, as well as below 900 m (around 170 μmol.kg^{-1}). Stratification is only partially found in the salinity profiles: lower concentrations at the surface (around 35.5 g.kg^{-1}) and below 400 m (less than 35.25 g.kg^{-1}) and higher concentrations between 100 m and 400 m (around 36 g.kg^{-1}).

In the intermediate layers, between 100 and 500 m, we notice a strong variability in the oxygen, and especially strong pulses of low values. We isolated two strong ~~deoxygenation~~ low oxygen events (~~D1 and D2~~O1 and O2) with values below 140 μ

mol.kg^{-1}. ~~D1~~ O1 is an event of about one month covering October 2015 with measurements between 150 μmol.kg^{-1} and 140 μmol.kg^{-1}. ~~D2~~ O2 is spread over two months from February to March 2016 with measurements lower than 130 μmol.kg^{-1}. The DOXY signatures of ~~D1 and D2~~ O1 and O2 do not correspond to the classical characteristics of the NCJ (Gasparin et al., 2011), whereas the float is exactly on its pathway. We therefore seek to know its origin. Based on the work of Gasparin et al. (2014) and Rousselet et al. (2016), we hypothesize that this signature originates from the NVJ waters whose theoretical and observed pathway is located 4^o further north (Fig. 5b). The figure of Appendix B shows the depth variability of the DOXY minimum of each profile during ~~D2~~ O2 and helps to understand the link between the ~~deoxygenation~~ low oxygen events and the properties of NVJ waters.

3.1.2 Thermohaline and circulation context

We focus on ~~D2~~ O2 that is longer and stronger than ~~D1~~ O1. The geostrophic velocity fields from AVISO (Fig. 5a) allow us to visualize the position of the float during ~~D2~~ O2 in relation to the surface circulation. We notice that, during the whole duration of ~~D2~~ O2, the float is located on the Queensland plateau where we can note that the deepest measurements are shallower than the parking depth (also visible in Figures 4a,b,c). This leads to short displacements over the whole event, making the interpretation of the results easier. We can identify a very large cyclonic structure to the east of the plateau centered at 156^{o}E, that we name C1, and a much weaker cyclonic structure, C2, located to the north-west of the plateau. Between them, we observe an anticyclonic structure, A, centered at 153^{o}E and stretching from 13^{o}S to 17^{o}S. The western branch of A (152^{o}E) forms a meridional path with southward velocities.

Using the HYCOM re-analysis, we can compare the AVISO observations to the modeled velocity field at different depths. At 300 m, the depth of the DOXY minimum, we can clearly identify structures C2 and A but C1 is harder to locate (Fig.5b). C1 may be located 1^o farther south. A is much more circular in the HYCOM re-analysis than in the AVISO surface data. These data also allow us to consider the densities of these water masses and thus enable us to track the potential NVJ waters down to the NCJ pathway. Figure 5b clearly shows that the NVJ waters can be associated with C2 for instance.

Otherwise, studying the AVISO product and HYCOM re-analysis for ~~D1~~ O1, we do not identify an eddy structure or a circulation shape that could explain that DOXY anomaly. Nevertheless, due to the large scale features of water masses and the low values of DOXY, observed in Figure 4c, we could hypothesize~~d~~ that such ~~deoxygenation~~ low oxygen events are related either to the intrusion of waters transported by mesoscale eddies or by NVJ meanders. Because we can observe such circulations with AVISO products, they definitely affect the surface layers and then impact the studied diazotrophic zones of the OUTPACE cruise. In the section 4.1, we will further discuss such aspects.

It should be noticed that it still remains difficult to interpret observations of different nature, i.e. from an Eulerian versus Lagrangian point of view, and that further work is required to ~~re~~place the float observations in their complete dynamical context.

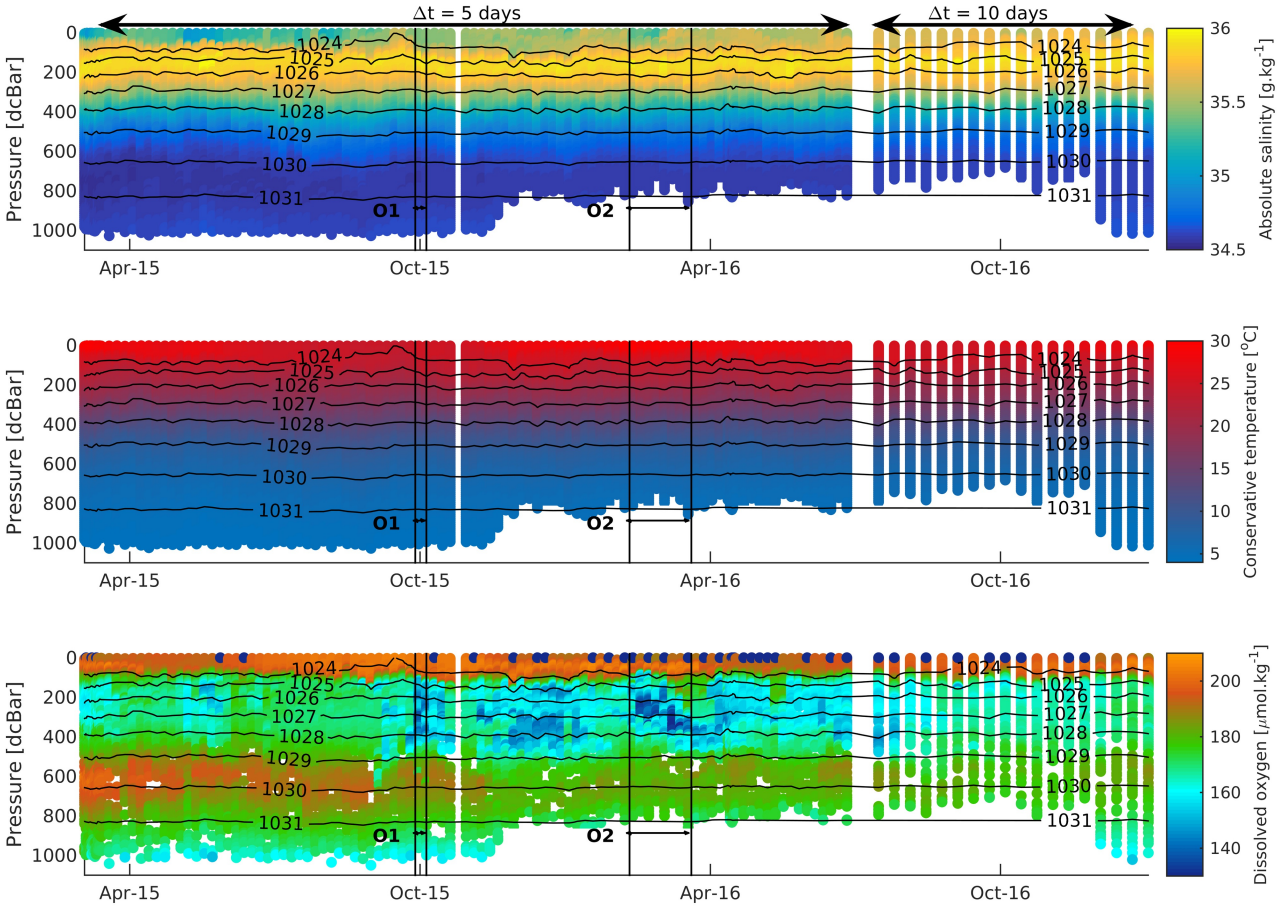

Figure 4. Profiles of float 656 over depth and time for (a) absolute salinity, (b) conservative temperature and (c) dissolved oxygen concentration. Every colored point corresponds to a measurement. The horizontal black lines indicate the isopycnals from 1024 to 1031 kg.m^{-3}. The vertical black lines indicate the limits of the ~~deoxygenation~~ low oxygen events ~~D1 and D2~~ O1 and O2. Over the top of the picture~~s~~ (a), Δt precises the two different sampling frequencies of the float.

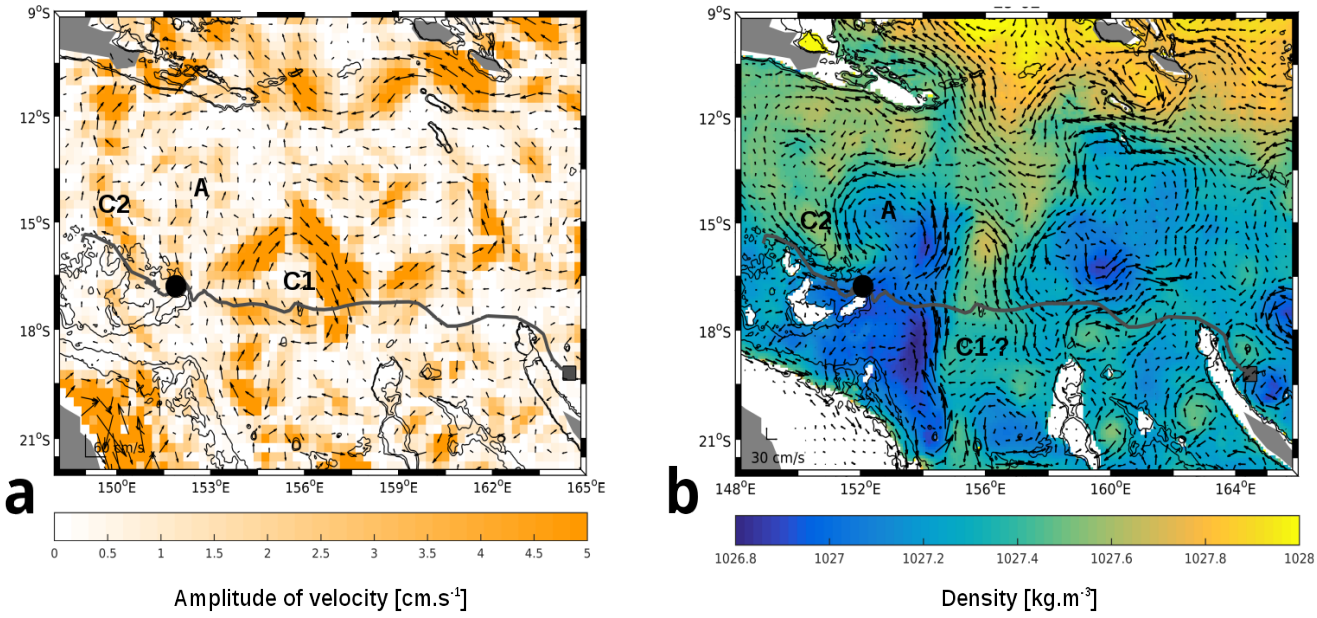

Figure 5. (a) Amplitude of surface geostrophic velocity on February 29th during ~~D2~~ O2, 2016 calculated from AVISO product ; (b) Density and velocity field at 300 m depth on February 29th during ~~D2~~ O2, 2016 calculated from HYCOM re-analysis. The gray line corresponds to the full trajectory of float 656 and the black point to the location of the float at the stated date. The black lines correspond to the bottom topography with 300 m and 1000 m depth.

3.2 Central Pacific Ocean

3.2.1 Float waves description and Doppler shift correction

In this part we focus on the trajectories of three OUTPACE floats : 660, 671 and 679 moving eastward and one THOT float : 687 moving westward. These floats were all deployed in spring 2015 and now show, after two years of drifting, zonal wavy trajectories (Fig. 2). We consider this group of OUTPACE floats distinctly from the THOT float because of their different directions. Then, we compare their respective float wave characteristics.

The wave characteristics of the two groups (Tab. 3) are clearly different: 71 days period and 159 km wavelength for the eastward group and 232 days period and 434 km wavelength for the westward float. Based on the couple ($\omega_{M\ell}$, $k_{M\ell}$) and following the method described in section 2.2, we first estimate the Eulerian characteristics of the theorical waves (ω_{Te},k_{Te} and ultimately ω_{TMe},k_{TMe}) that better fit the floats.

To simplify the presentation, we only use the 660 and 687 float waves properties. We choose these two floats because they are the ones with the most regular trajectories (neither going northward like float 679 or southward like float 671). As explained in section 2.2, since the two regions of minima cross, the two observed float waves can be the signature of a single theoretical

Table 3. Period T and wavelength λ of the float waves. The mean, standard deviation and extrema values are calculated for the eastward floats : 660, 671 and 679 (top of the table). Then details are given for each floats: dates, geographical area, half periods, half wavelengths and corresponding mean and standard deviation values for T and λ.

EASTWARD (stat)

	Lat [^{o}S]	Lon [^{o}W]	T [days]	λ [km]
Mean $\pm$ std	18.8 ± 0.9	160.8 ± 3.4	71 ± 21	159 ± 74
[min;max]	[20.7 ; 17.8]	[168.2 ; 156.7]	[40 ; 120]	[42 ; 275]

EASTWARD (details)

Float	Date	Lat [^{o}S]	Lon [^{o}W]	$T/2$ [days]	$\lambda/2$ [^{o}]	$\bar{T}$ [days]	$\bar{\lambda}$ [km]
660	Feb 7th, 2016 to Nov 21st, 2016	[18.6 ; 17.8]	[161.4 ; 156.7]	35	0.7	82 ± 20	138 ± 74
				42	1.4		
				40	0.5		
				30	0.2		
				35	0.8		
				45	0.6		
				60	0.5		
671	Jul 8th, 2015 to Feb 3rd, 2016	[18.9 ; 18.1]	[162.6 ; 157.8]	30	0.6	70 ± 11	201 ± 74
				30	1.1		
				40	1.2		
				40	0.4		
				40	1.3		
				30	1.0		
679	Aug 13th, 2016 to Dec 31st, 2016	[19.2 ; 17.3]	[161.5 ; 158.8]	20	0.7	56 ± 26	127 ± 32
				20	0.6		
				30	0.7		
				20	0.3		
				50	0.6		

WESTWARD (details)

687 (THOT)	Jul 18th, 2015 to Oct 31st, 2016	[20.9 ; 19.2]	[157.8 ; 150.1]	65	2.5	232 ± 93	434 ± 159
				95	1.2		
				173	2.8		
				130	1.5		

wave. Considering this hypothesis, we find that this wave is defined in the ranges from 0 to 0.075 rad.day^{-1} for the frequency and from -0.04 to 0.02 rad.km^{-1} for the wavenumber (Fig. 6a). In order to get a better resolution and minimize the calculation time, we make a zoom on those ranges of frequencies and wavenumbers before doing the minimum calculation. We set a resolution of $5 \cdot 10^{-5}$ rad.day^{-1} and $5 \cdot 10^{-5}$ rad.km^{-1} and find 8083 minima, mostly in the westward region (Fig. 6b).

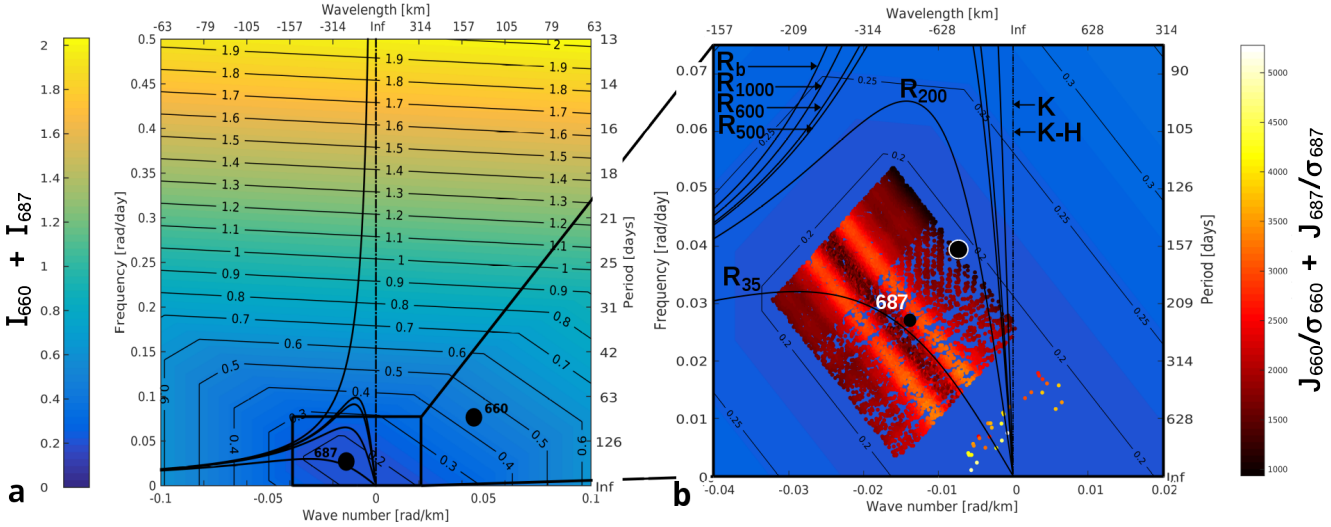

Figure 6. Difference between observed Lagrangian float wave characteristics and Lagrangian theoretical wave ones (index **I**, left colorbar) for (a) the sum of floats 660 and 687 and (b) the associated minimum calculations (normalized index **J**, right colorbar) with regard to dispersion equations of Rossby wave (solid line), Kelvin wave (dotted line), Kevin-Helmholtz instability wave (break line). Subscript b means a barotropic case, ~~200~~ subscripts with number means a baroclinic case with a stratification at ~~200 m~~ the depth of this number. The negative wavelength describes a westward wave. Black dots indicate the observed Lagrangian parameters, on (b) only 687 ones are inside the range; the red dots show the minima of the index hence the best parameters that can explain both trajectories; the black dot circled of white is the couple (ω_{TMe} , k_{TMe}) that better fits the 660 and 687 float trajectories.

In order to compare the couples (ω_{Te} , k_{Te}) to classical oceanic waves, we calculate the dispersion equation of Kelvin and Rossby in a vertical baroctropic case, Kelvin-Helmholtz instability wave in a two layers case and Rossby waves in several baroclinic cases (the different cases are explained in Appendix D). We observe that the characteristics of the Kelvin and Kelvin-Helmholtz instability waves are not in the same ranges as the ones of the couples we want to identify. Rossby waves (**R**) are the ones that better fit them. The barotropic case $\mathbf{R_b}$ is out of range but most solutions are located around the curves of the baroclinic cases with a thermocline at 35 m ($\mathbf{R_{35}}$) and 200 m ($\mathbf{R_{200}}$).

Using the J index, we are able to select the couple that better fits both the 660 and the 687 float trajectories. The results give us a wave of 160 days period and 855 km westward wavelength, the validity of this result will be discussed in the next section. Figure 7 illustrates the agreement between the observed and the reconstructed trajectories obtained from it. Obviously, some other processes with small-scale signatures also influence the observed float trajectories. Nevertheless, a single wave, added to the float respective zonal background currents, can mainly explain the two float trajectories that would otherwise be classified,

at first sight, as behaving differently. Such observations of a potential plane wave have been rarely highlighted so far, and even less at such depth.

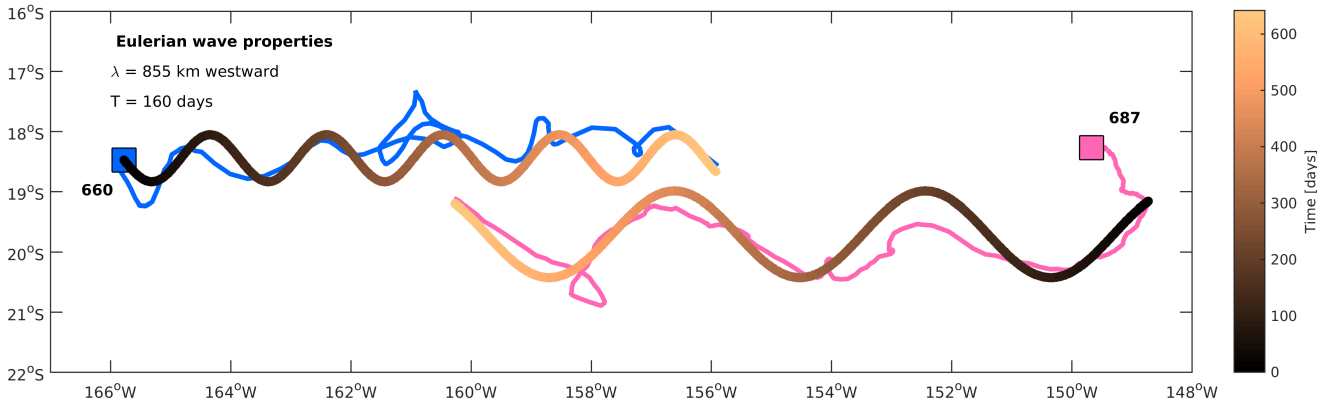

Figure 7. Best analytical solution of Lagrangian trajectories for both floats 660 and 687. The blue line refers to float 660, the pink one to float 687, the squares refer to their initial location. The black to brown lines refers to the best theoretical solution with a time step of one day.

With the best fitting wave characteristics (ω_{TMe} , k_{TMe}), we can calculate the phase speed of the wave and the diagnostic ε for each float. Hence $c = -6.2$ cm.s^{-1}, $\varepsilon_{660} = -0.27$ and $\varepsilon_{687} = 0.31$. As expected, $\varepsilon_{660} < 0$ meaning the float 660 is in a retrograde context and $\varepsilon_{687} > 0$ meaning the float 687 is in a retrograde one. The value of ε is still very week ($-1 < \varepsilon < 1$) in both context. This attest that we are in a case of no-trapping of the float by the wave (Flierl, 1981).

3.2.2 Thermohaline and circulation context

Using HYCOM re-analysis, we are able to ~~re~~place the trajectory of the floats into the circulation at 1000 m depth. Figures 8 a and b highlight the current striations as mentioned in the introduction. We observe that the modeled striations have, on average, widths of 1^o to 1.5^o of latitude, which are smaller than those observed by Ollitrault and Colin de Verdière (2014) (Fig. 1c). The mean shear of zonal velocity observed by the floats 660 and 687 is equal to 4.2 cm.s^{-1} (zonal velocities used in the Appendix A for case b). ~~We note a difference between the Eulerian modeled zonal velocities and the Lagrangian zonal velocities of the floats, which is not surprising taking into account the Eulerian versus Lagrangian description.~~

We also use the HYCOM re-analysis fields of temperature and salinity in order to calculate the density context of the studied area (Fig. 8c). The two floats 660 and 687 are both at the interface of two different water masses : the northern one with a density around 1032 kg.m^{-3} and the southern one with a density around 1031.85 kg.m^{-3}. This corresponds to a density difference of 0.15 kg.m^{-3} in a 2^o latitudinal range with the isopycnals being deeper southward. The front location, shape and intensity are variable with some extreme events of displacement or intensity, ~~like~~ such as on November 13th, 2015 (Fig. 8d). But the front ~~globally~~ usually stays a zonal boundary located around 20^oS, ~~like~~ such as on September 29th, 2015 (Fig. 8c).

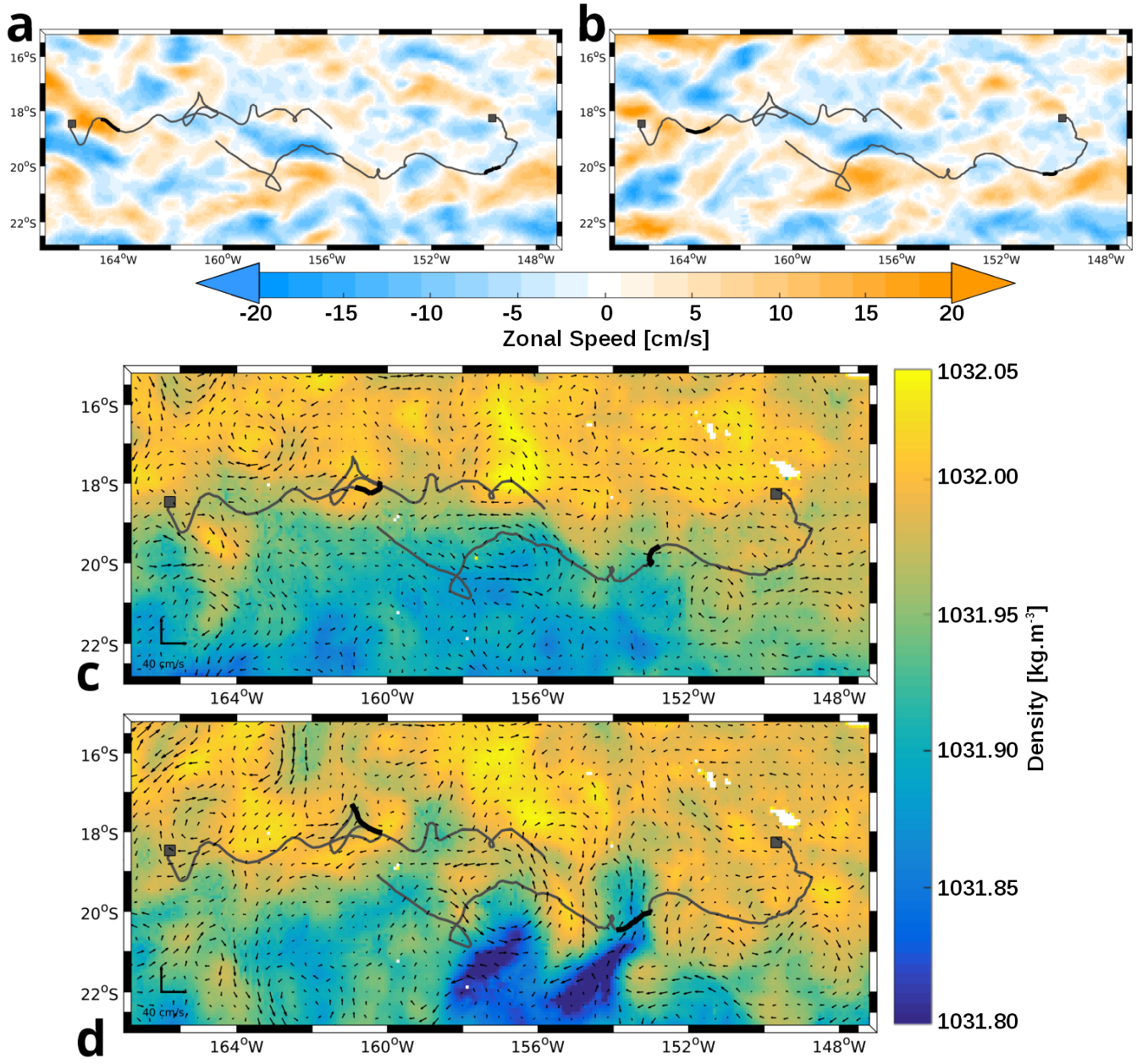

Figure 8. (a,b) Zonal velocity (positive for eastward velocity) at 1000 m depth on (a) July 1st, 2015 and (b) July 16th, 2015 from HYCOM re-analysis; (c,d) density and velocity field at 1000 m depth on (c) September 29th, 2015 and (d) November 13th, 2015 calculated from HYCOM re-analysis; The gray lines correspond to the full trajectory of the floats and the black portions to the location of each float at the stated date and on the 15 following days.

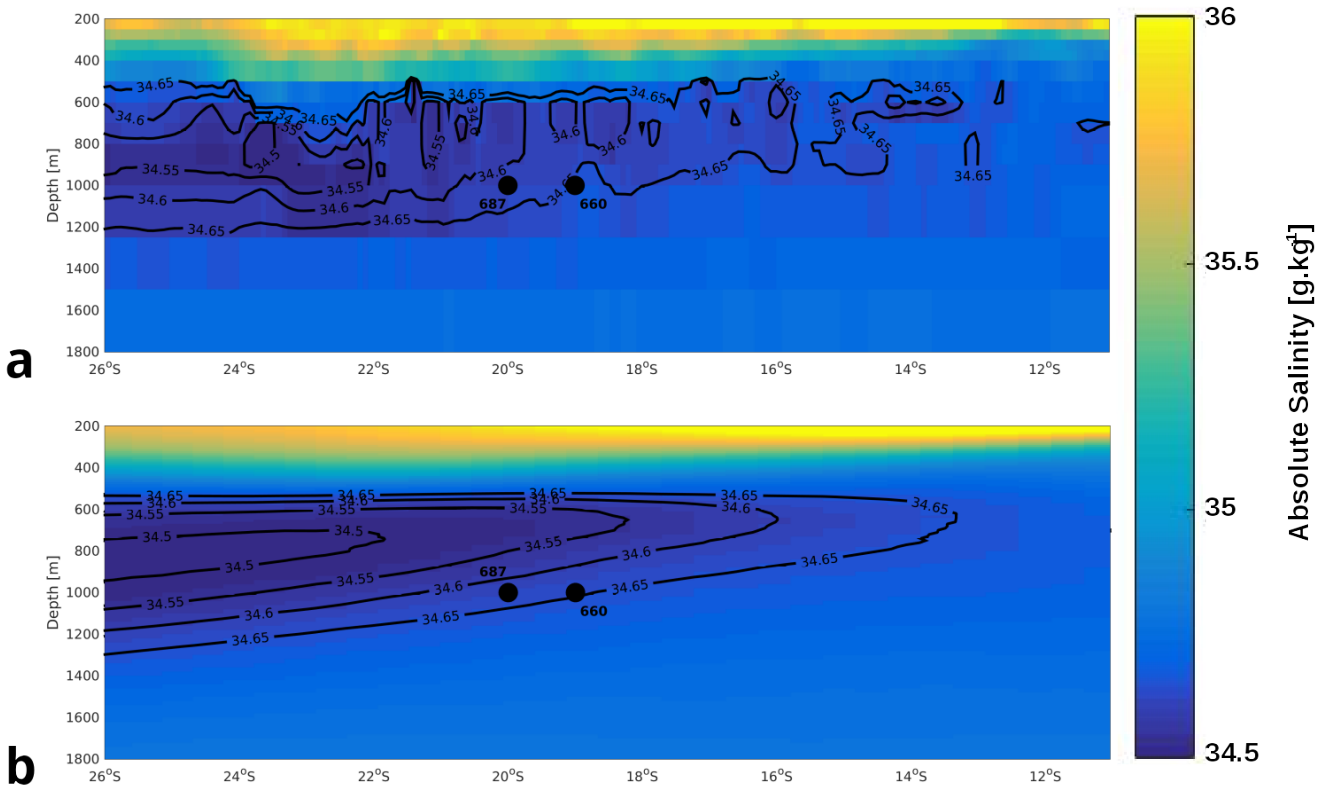

Figure 9. Absolute salinity meridional section at 157^{o}W calculated from (a) HYCOM re-analysis on November 13th, 2015 and (b) ISAS13 atlas for November seasonal climatology. Black dots indicate the mean location of the floats.

Meridional cross-sections of HYCOM re-analysis (Fig. 9a) show a salinity gradient in the intermediate waters, between 500 m and 1200 m. We can note the meridional gradient of salinity at the parking depth of the float, around ~~900~~ 1000 m: saltier (35 g.kg^{-1}) north of 19^o and less salty (34.5 g.kg^{-1}) south of 19^o. These values are also observed in the ISAS13 climatology (Fig. 9b). To quantify the meridional slope of this front, we analyze the depth of the isopycnal 1031.95 kg.m^{-3} (average between the two sides of the front) from 147^{o}W to 167^{o}W and from 15^{o}S to 25^{o}S. Then we perform a linear regression on the isopycnal depths in their steepest part between 17^o S and 22^o S. We can obtain, for example, low values: 3.8 m per degree of latitude on November 13th, 2015 (Fig. 8d), average values: 4.2 m per degree of latitude on September 29th, 2015 (Fig. 8c), and what we call extreme values such as 26.9 m per degree of latitude on November 13th, 2015. To verify if the meridional slope varies over the year, we have done the calculations for the complete ISAS13 climatology (Tab. 4). These slope values range from a minimum of 3.9 m per degree of latitude in June to a maximum of 4.5 m per degree of latitude in February. They do not exhibit any apparent annual cycle and the density front appears to be a permanent feature.

Table 4. Meridional slope of the isopycnal 1031.95 kg.m^{-3} in the monthly climatology of the ISAS13 atlas.

Month	Jan.	Feb.	Mar.	Apr.	May	Jun.	Jul.	Aug.	Sep.	Oct.	Nov.	Dec.
Slope [m.^{o}lat^{-1}]	4.3	4.5	4.2	4.0	4.3	3.9	4.3	4.0	4.0	4.4	4.1	4.4

Otherwise, we note that, from May to July 2015, a cyclonic eddy (centered about 165^{o}W and 18.5^{o}S on Figures 8a,b) crossed the trajectory of float 660. Hence, ~~it can not be ruled out that this eddy could have influenced~~ it is likely that this eddy influenced the beginning of float 660 trajectory and produced a certain variability in its oscillations. Concerning the trajectory of float 687, we do not observe any stable eddy structure around it during ~~all its studied~~ the whole period. That explains why we did not choose to interpret the wavy float trajectories with the unique hypothesis of eddy impacts.

4 Discussion

4.1 Coral Sea

Analyzing the DOXY measurements of float 656, we were able to describe two distinct events with well marked oxygen minima (~~D1 and D2~~ O1 and O2, Fig. 4c) between 150 m and 400 m depth, i.e. near the upper part of the main thermocline. Inspired by the previous study of Rousselet et al. (2016), we associate these oxygen minima to the NVJ waters, much ~~more deoxygenated~~ less oxygenated than those of the NCJ. We propose that the NVJ waters were indeed transported by mesoscale eddies. To support this hypothesis, we compare the geostrophic currents at the surface with AVISO data and also use the HYCOM re-analysis at 300 m. ~~Even if the comparison was not clear enough for D1 to be fully conclusive, i~~ In the case of ~~D2~~ O2 we have been able to identify a cyclonic structure (C2, Fig. 5) and an anticyclonic structure (A1) in the two sets of data. These vortex structures are involved in the transport of NVJ waters southward to the NCJ pathway. Maps of density resulting from the HYCOM re-analysis inform us about the nature of the cores of these vortex structures. Structure A carries NCJ waters while C2 transports NVJ waters. This clear difference forms a density gradient of 0.6 kg.m^{-3} over 3^o of longitude approximately. From this, we can hypothesize that the signature of the oxygen minimum is due to C2 carrying NVJ waters in its core. ~~Otherwise,~~ Looking at the evolution of the velocity field, we note that the common branch of C2 and A forms a local southward current exactly toward the position of the float 656. ~~Hence, we can also make a second hypothesis that the NVJ waters could be carried by the northern branch of A and then be transported southward thanks to the current located between A to the east and C2 to the west.~~ This current could also play a role in the transport of NVJ waters. Hence, we propose a second hypothesis of an edge transport for the NVJ waters going south. These waters could be first carried by the northern edge of A and then be transported southward thanks to the current located between A to the east and C2 to the west. The first hypothesis fits the results of Rousselet et al. (2016), with the difference that the structure transporting NVJ waters is cyclonic and not anticyclonic. Hence the two possibilities that we propose widen the ~~comprehension~~ understanding of the connection processes between the NVJ and the NCJ and ~~claim for the~~ suggest that there be an explicit consideration of mesoscale ~~eddies~~ eddy variability in future modeling approach.

Thanks to the analysis of the OUTPACE observations, Fumenia et al. (2018) hypothesize that the location of nitrogen sources and sinks could be decoupled. Thus, the authors propose that the transport of rich nitrogen thermocline waters from N_2 fixation could join the subtropical gyre through the EAC (Fig. 1a). Bouruet-Aubertot et al. (2018) also observe a westward increase of turbulence~~s~~ during OUTPACE. This leads to a strong turbulent regime in the Melanesian Archipelago, located at the entrance of the Coral Sea, highly visible in nitrogen measurements during the long term stations. Extending these conclusions to the Coral Sea set a favorable context to the exchanges between NVJ and NCJ. Specific exchanges from NVJ to NCJ ~~could~~ would, then, strengthen the recirculation in the subtropical gyre of rich nitrogen waters. Thus understanding their dynamics could help us to better understand their impact on the propagation of biogeochemical components.

4.2 Central Pacific Ocean

The trajectories of OUTPACE and THOT Argo floats give us two groups of float waves with different characteristics. Whereas the long-term mean displacement of the floats could be explained by the presence of alternating striations as deduced from the displacement of the Argo floats at their parking depth, we focused on their quite-surprising oscillation characteristics. In this study, we show that their oscillating trajectories can be caused by a single theoretical wave of 160 days period and 855 km wavelength superimposed to the zonal background current. Focusing on Figure 7, the fit over the trajectory of float 687 is very convincing. It is less so for float 660. We can explain this by recalling that the beginning of the 660 trajectory is, partially or entirely, influenced by an eddy passing through (Fig. 8a,b). Another explanation could be that, in Eq. 4 and 5, we consider the zonal velocity u_0 as constant during the entire simulations. But a variable zonal velocity is likely to strongly impact the float trajectory. We detail this ~~point~~ sentence with two examples that can be observed on the 660 and 687 trajectories, respectively. The first one takes place on the 660 trajectory between 159^{o}W and 158^{o}W (Fig. 7). It happens when the zonal velocity decreases while keeping the same direction eastward (Fig. 10a). This leads to a smaller local wavelength. The second one takes place on the 687 trajectory around 158^{o}W. It happens when the zonal velocity changes direction, from westward to eastward (Fig. 10b). This leads to a loop in the Lagrangian trajectory. The impact of a variable zonal velocity does not refute our hypothesis of a single wave influencing the two floats 660 and 687, but questions the precision of the values found (ω_{TMe} , k_{TMe}). The same comment also applies to the description of the couples $(\omega_{M\ell}$, $k_{M\ell})_{660}$ and $(\omega_{M\ell}$, $k_{M\ell})_{687}$ that could not be performed using a Fourier transformation or a wavelet analysis due to the short duration of the float data time series compared to the sampling frequency. Using a plane wave description is a source of inaccuracy because such wave are rarely observed in open ocean studies. Some propositions for further analyses are detailed in the next section.

Based on the HYCOM re-analysis, we confirm that both the 660 and the 687 floats move in shear environments. This shear context is supported by a density front which is permanent all year round. This front could be associated with the base of the northern edge of the Antarctic Intermediate Waters that reach this latitude near our study zone (Bostock et al., 2013). The best fitting wave that we found is close to a Rossby wave in a baroclinic ocean case with a thermocline at 200 m. This case is close to the real context of the studied zone where the upper thermocline waters are located around 200 m (GLODAPv2 database, Fumenia et al., 2018). Moreover, this zone is precisely located where Rossby waves are frequently found and their signatures can be observed through sea level anomalies (Maharaj et al., 2007). Those arguments strengthen the hypothesis of

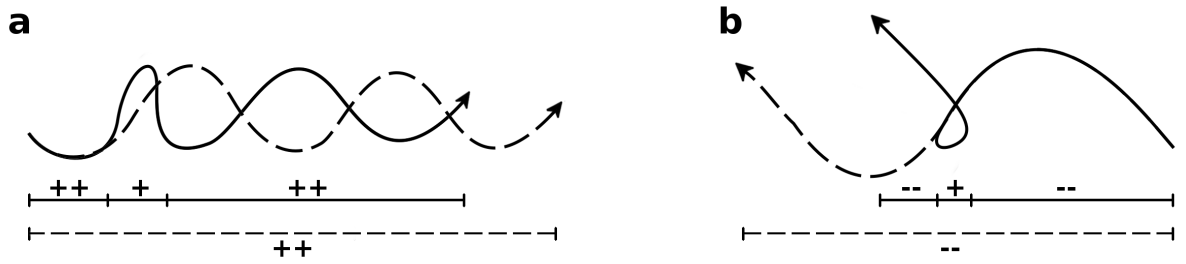

Figure 10. Sketch explaining the influence over a Lagrangian trajectory of (a) a zonal velocity decrease like in the 660 trajectory and (b) a zonal velocity inversion like in the 687 trajectory. The horizontal dash lines refer to the trajectories influenced by a wave with a constant zonal velocity. The horizontal solid lines are segmented with the periods associated to the sign above them. The signs indicate the strength and the direction of the zonal velocity : ++ for strong eastward, + for weak eastward and - - for strong westward.

a Rossby wave close to 160 days period and 855 km wavelength. These observations lead to a large discussion of the possible interactions between waves and intermediate flows.

Such processes could have a significant impact on the sampling strategy of intermediate waters by shifting the front location hundreds of kilometers from its mean location. OUTPACE sampling strategy during long duration stations keep sampling within Rossby radii of each station ensuring to generally follow the same water mass (de Verneil et al., 2017a). ~~It also questions the use of averaged datasets of intermediate flows that do not account for such processes.~~ More generally, this study considers the trajectories of floats worth being studied by themselves and beckons the development of different methodologies to exploit such measurements in the future.

5 Conclusions & Perspectives

In this study, we have been able to highlight different pattern of the intermediate flows in the South Tropical Pacific Ocean through the description of the characteristic trajectories of some autonomous floats of the international Argo project deployed during the OUTPACE cruise (Moutin et al., 2017) and by the THOT project (Martinez et al., 2015).

Relying on the measurements of dissolved oxygen concentration (DOXY) onboard a PROVBIO float, we have found a meridional southward transport of NVJ waters by mesoscale eddies causing oxygen minima intrusions in the NCJ pathway around 300 m depth. Our results widen those of Rousselet et al. (2016), since we show that the transport can occur inside the core of a cyclonic eddy or between a couple of anticyclonic and cyclonic structures. Moreover, the hypothesis that the waters can be transported on the edge of several eddies is a new proposed pathway for NVJ waters ~~, as far as we know.~~ To ensure the mechanisms of this meridional transport, the fronts between the described cyclonic and anticyclonic eddies could be studied using Finite Size Lyapunov Exponents calculations. These calculations could be applied to both AVISO and HYCOM data to provide information at different depths. Another solution is to ~~re~~place the Lagrangian observations in their finer circulation context; a study based on dynamic attractors (Mendoza and Mancho, 2010) could be useful to test our assumptions. Otherwise,

since DOXY is the parameter that can differentiate NVJ from NCJ, ~~recourse~~ resort to biogeochemical models could help visualizing and studying the connection between the NVJ and the NCJ. Finally, how these differences in the partition between the jets influence the other biogeochemical parameters and the phytoplankton biology remain to be specifically investigated.

In addition to the description of water mass~~es~~ properties, we observe dynamical features such as wavy float trajectories in the central part of the Pacific Ocean corresponding to a circulation mechanism occurring near 1000 m depth (parking depth). The shear of zonal velocity ($\Delta u = 4.2$ cm.s^{-1} for the floats) associated with a permanent density front ($\Delta \rho = 0.15$ kg.m^{-3}) form a favorable ~~context~~ environment for the development of instabilities. ~~Correcting the impact of the Lagrangian observation~~ In order to convert Lagrangian wave observations into Eulerian ones in a simplified case, we concentrated on two floats, heading in opposite zonal directions and hence providing both cases of prograde and retrograde motions. Moreover, we chose two PROVBIO floats in order to assure that their motions are representative of depth dynamics (as explained in Section 2.1). We found that their behaviors, apparently opposite, could be described with a single wave of 160 days period and 855 km wavelength heading westward. This couple of parameters can be identified as a Rossby wave in a baroclinic context for a two layers ocean with a thermocline at 200 m. To get a better float wave description, using Fourier transformation or a wavelet analysis, would require ~~to wait until the time series are longer~~ a longer time series. In addition, to refine the method and results, we suggest to improve the Lagrangian simulation, that we used to fit the trajectories, by taking into account the temporal variations of zonal velocity for each float. Another approach could also be made with an inverse model. Whereas, to improve the comparison to classical waves, the dispersion equation of a Rossby wave could be calculated in the 3D context of the interface between Antarctic Intermediate Waters and the North Pacific Deep Waters. The baroclinic instability of the density front is an alternative hypothesis that could also be considered in order to explain the float trajectories. Because the front is permanent, other immersions of floats at different latitudes on two meridians enclosing the study zone would also consolidate the observations of this process. Nevertheless, all these perspectives are beyond the scope of this paper and will be considered in future works.

~~Thanks to this study, we underline the importance of eddies as well as waves in~~ This study underlines the importance of waves in addition to eddies for the mesoscale dynamics of intermediate flows. We stress the importance of taking into account individual float measurements and trajectories in further studies in order to better understand water mass transport, mixing processes and their potential impacts on biogeochemical cycles.

Appendix A: Wave fit on float trajectories

Table A1. Characteristics of the theoretical wave that better fit both 660 and 687 float trajectories for different zonal speed cases and resolution. Case a) refers to the global mean zonal velocity of each float from the first cycle to the last one for 660 trajectory and from the 58th cycle to the last one for 687 trajectory (see section 2.2). Case b) refers to the mean of all the measured zonal velocities for each float. Case c) refers to the mean of all floats (i.e. the mean of all the values obtained in case b).

Case	Zonal velocity		Identical resolution	Potential fits	T_{TMe}	λ_{TMe}	φ_{TMe}	Propagation
	660	687	for $\Delta\omega$ and Δk					
	[cm/s]		[rad/day & rad/km]	[#]	[days]	[km]	[rad]	
	1.65	-1.93	$5 \cdot 10^{-4}$	107	126	449	0.7π	Westward
	1.65	-1.93	$2 \cdot 10^{-4}$	502	126	449	0.7π	Westward
a)	1.65	-1.93	$1 \cdot 10^{-4}$	2054	121	422	0.7π	Westward
	1.65	-1.93	$7 \cdot 10^{-5}$	4592	121	417	-0.5π	Westward
	1.65	-1.93	$5 \cdot 10^{-5}$	8083	160	855	-0.5π	Westward
	1.83	-2.34	$5 \cdot 10^{-4}$	121	182	393	0.1π	Westward
	1.83	-2.34	$2 \cdot 10^{-4}$	715	150	308	-0.5π	Westward
b)	1.83	-2.34	$1 \cdot 10^{-4}$	2945	169	332	0.1π	Westward
	1.83	-2.34	$7 \cdot 10^{-5}$	5801	147	306	0.1π	Westward
	1.83	-2.34	$5 \cdot 10^{-5}$	11593	169	332	0.1π	Westward
	2.09	2.09	$5 \cdot 10^{-4}$	2731	483	838	0.3π	Eastward
	2.09	-2.09	$2 \cdot 10^{-4}$	16903	204	383	-0.1π	Westward
c)	2.09	-2.09	$1 \cdot 10^{-4}$	67591	-	-	-	-
	2.09	-2.09	$7 \cdot 10^{-5}$	137567	-	-	-	-
	2.09	-2.09	$5 \cdot 10^{-5}$	270730	-	-	-	-

Appendix B: Profiles of float 656 during ~~D2 deoxygenation event~~ O2 low oxygen event

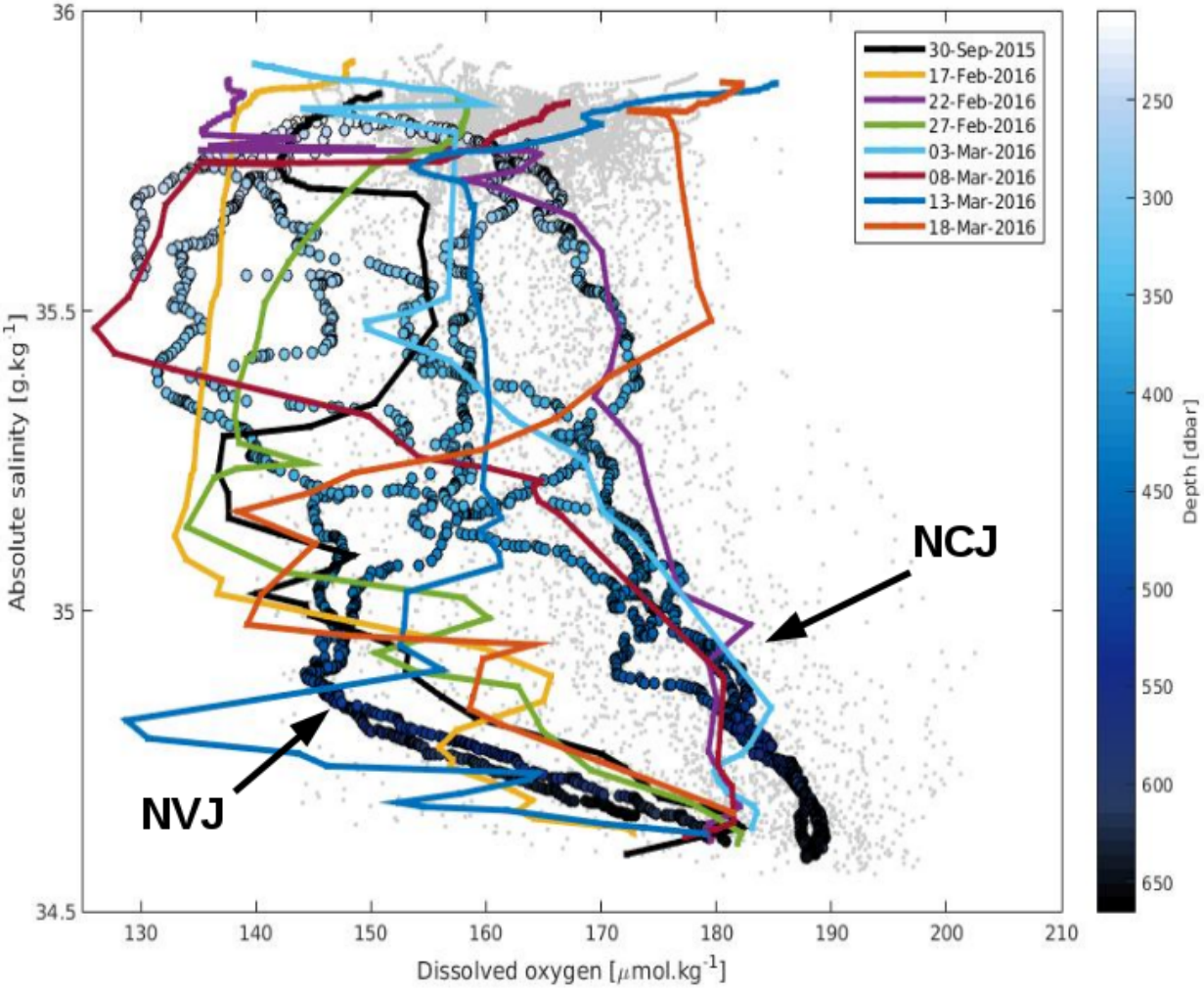

Figure B1. DOXY versus absolute salinity profiles of float 656 during ~~D2~~ O2 (colored lines) compared to characteristic NCJ and NVJ profiles made during BIFURCATION cruise (scaled dots). The grey dots are the other measurements made by float 656. All the profiles are shown from the isopycneal 1026 kg.m^{-3} to the one 1030 kg.m^{-3} (i.e. between 200 and 650 m depth, approximately).

Appendix C: Argo float profiles versus HYCOM re-analysis profiles

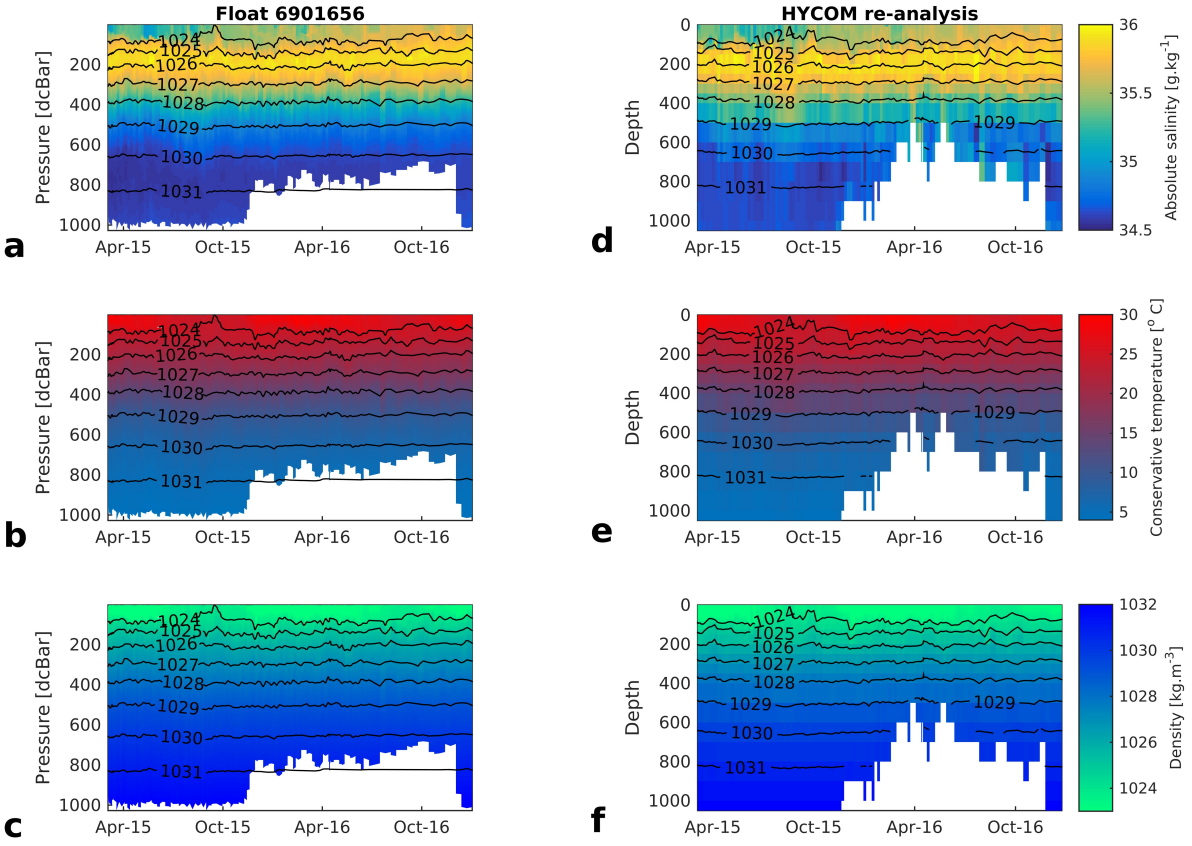

Figure C1. Profiles of (left side) float 656 and (right side) corresponding data from HYCOM re-analysis over depth and time for (a,e) absolute salinity, (b,f) conservative temperature and (c,g) density. Every colored point corresponds to a measurement. The black lines indicate the isopycnals from 1024 to 1031 kg.m^{-3}.

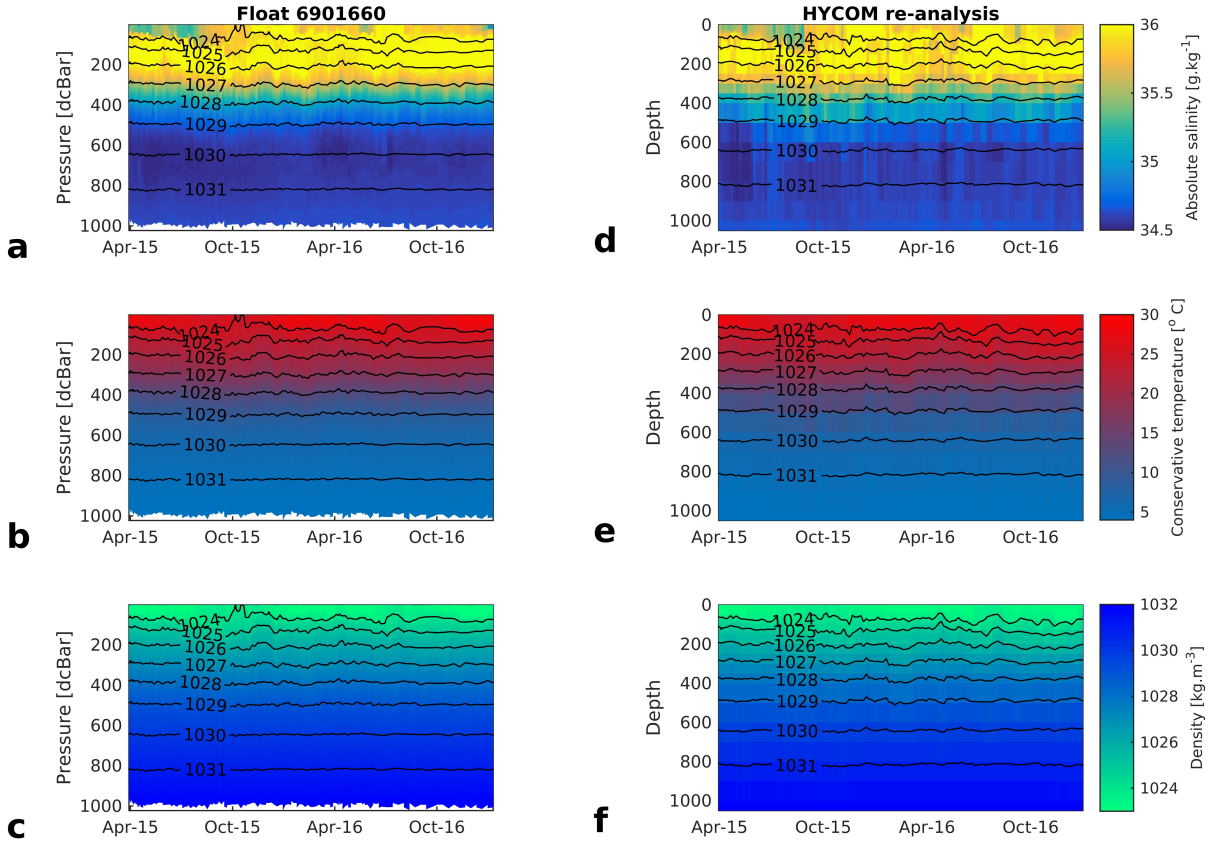

Figure C2. Profiles of (left side) float 660 and (right side) corresponding data from HYCOM re-analysis over depth and time for (a,e) absolute salinity, (b,f) conservative temperature and (c,g) density. Every colored point corresponds to a measurement. The black lines indicate the isopycnals from 1024 to 1031 kg.m^{-3}.

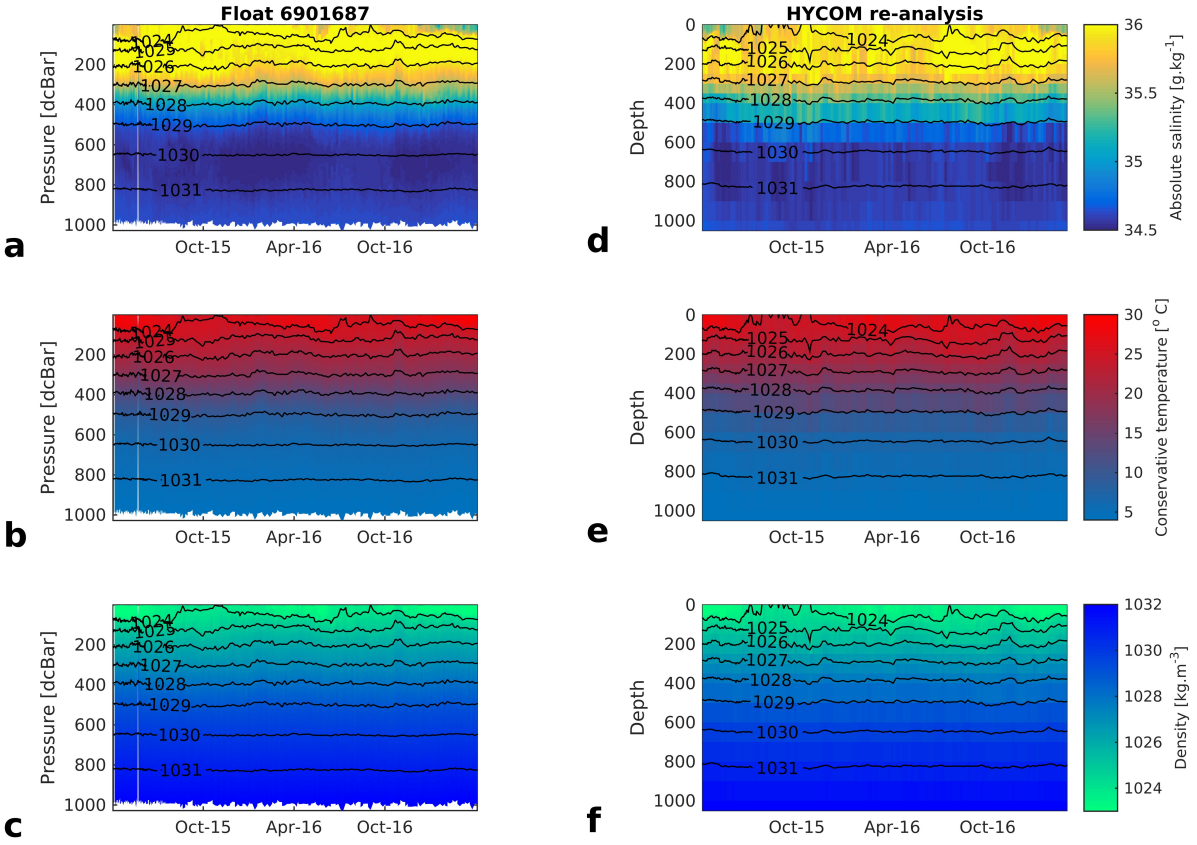

Figure C3. Profiles of (left side) float 687 and (right side) corresponding data from HYCOM re-analysis over depth and time for (a,e) absolute salinity, (b,f) conservative temperature and (c,g) density. Every colored point corresponds to a measurement. The black lines indicate the isopycnals from 1024 to 1031 kg.m^{-3}.

Appendix D: Linear Rossby wave dispersion equation

We describe the Rossby wave in different cases. First, in a barotropic ocean, so the dispersion equation is:

$$\omega = -\beta \frac{k}{k_H^2} \tag{D1}$$

with ω the frequency, k the wavenumber and k_H the horizontal wavenumber of the wave and β the Rossby parameter. We place ourselves at 19^{o}S, so $\beta = 2.1 \cdot 10^{-11}$ m^{-1}.s^{-1} . In our study we are not able to estimate the value of the meridional wavenumber, hence we neglect it and consider that $k_H = k$ (Maharaj et al., 2007 also use this hypothesis in their study for calculation purpose). The equation becomes:

$$\omega = \frac{\beta}{k} \tag{D2}$$

Second, we take a baroclinic ocean with two layers separated by the thermocline. Still considering $k_H = k$, the dispersion equation is:

$$\omega = \frac{-\beta k}{k^2 + \frac{f_0^2}{c^2}} \tag{D3}$$

with c the phase speed, f_0 the Coriolis parameter at 19^{o}S equal to $-4.7 \cdot 10^{-5}$ s^{-1} . In this case the phase speed of the wave is expressed by the following equation:

$$c^2 = \frac{g\,\Delta\rho\, h_1 h_2}{\rho_2 h_1 + \rho_1 h_2} \tag{D4}$$

with ρ_1 and ρ_2 respectively the densities of the upper and lower ocean layer, $\Delta\rho = \rho_2 - \rho_1$ and h_1 and h_2 the corresponding height of the layers. Using the climatology of ISAS13 atlas and HYCOM re-analysis we make the calculations for four different cases (Tab. D1).

Table D1. Characteristics of the layers for the baroclinic cases of the Rossby wave calculation.

Name	Based on	h_1	h_2	ρ_1	ρ_2
		[m]		[kg.m^{-3}]	
$\mathbf{R_{35}}$	HYCOM	35	4965	1025	1032
$\mathbf{R_{200}}$	HYCOM	200	4800	1026	1032
$\mathbf{R_{500}}$	HYCOM & ISAS13	500	4500	1027	1032
$\mathbf{R_{600}}$	HYCOM & ISAS13	600	4400	1027	1032
$\mathbf{R_{1000}}$	HYCOM & ISAS13	1000	4000	1032	1038.5

Acknowledgements. Special thanks to the officers and crew of the R/V L'Atalante who operated the OUTPACE cruise (http://dx.doi.org/10.17600/15000900). The Argo data were collected and made freely available by the International Argo Project and the national programs

that contribute to it (http://www.argo.ucsd.edu, http://argo.jcommops.org). Argo is a pilot program of the Global Ocean Observing System. The altimeter products were produced by Ssalto/Duacs and distributed by Aviso, with support from CNES (www.aviso.altimetry.fr/duacs/). The HYCOM simulation and re-analysis are sponsored by the National Ocean Partnership Program (hycom.org). Thanks to Luiz Neto for developing a float profile toolbox, Alain Fumenia for the oxygen calibration of the OUTPACE floats and Fabienne Gaillard for ISAS analysis. The authors are grateful for the support of the OUTPACE project (PIs: Thierry Moutin and Sophie Bonnet) funded by the French research national agency (ANR-14-CE01-0007-01), the LEFE-CyBER program (CNRS-INSU), the GOPS program (IRD), the European FEDER Fund under project 1166-39417, and TOSCA/CNES (PI A.Doglioli, BC T23 ZBC 4500048836). We also thank ERC Remocean, the LEFE and MOM programs, as well as the Contrat de Projets Etat - Polynésie française for their financial supports to the THOT project lead by Elodie Martinez (IRD). Simon Barbot thanks the Physics team of MIO and the OUTPACE project for the funding of his internship, as well as the LATEX project (PIs: Anne Petrenko and Frédéric Diaz) for complementary support. Finally, the authors thank Xavier Carton for his proof-reading and comments as well as Kelvin Richards and the two anonymous referees for theirs constructive comments.

References

Belmadani, A., Concha, E., Donoso, D., Chaigneau, A., Colas, F., Maximenko, N., and Di Lorenzo, E.: Striations and preferred eddy tracks triggered by topographic steering of the background flow in the eastern South Pacific, Journal of Geophysical Research: Oceans, 122, 2847–2870, 2017.

Benavides, M., Berthelot, H., Duhamel, S., Raimbault, P., and Bonnet, S.: Dissolved organic matter uptake by Trichodesmium in the Southwest Pacific, Scientific reports, 7, 2017.

Bishop, J. K. B. and Wood, T. J.: Year-round observations of carbon biomass and flux variability in the Southern Ocean, Global Biogeochemical Cycles, 23, https://doi.org/10.1029/2008GB003206, http://dx.doi.org/10.1029/2008GB003206, gB2019, 2009.

Bonnet, S., Caffin, M., Berthelot, H., and Moutin, T.: Hot spot of N2 fixation in the western tropical South Pacific pleads for a spatial decoupling between N2 fixation and denitrification, Proceedings of the National Academy of Sciences, 114, E2800–E2801, 2017.

Boss, E., Swift, D., Taylor, L., Brickley, P., Zaneveld, R., Riser, S., Perry, M., and Strutton, P.: Observations of pigment and particle distributions in the western North Atlantic from an autonomous float and ocean color satellite, Limnology and Oceanography, 53, 2112–2122, 2008.

Bostock, H. C., Sutton, P. J., Williams, M. J., and Opdyke, B. N.: Reviewing the circulation and mixing of Antarctic Intermediate Water in the South Pacific using evidence from geochemical tracers and Argo float trajectories, Deep Sea Research Part I: Oceanographic Research Papers, 73, 84–98, 2013.

Bouruet-Aubertot, P., Cuypers, Y., Le Goff, H., Rougier, G., Picherall, M., Doglioli, A. M., Yohia, C., de Verneil, A., Caffin, M., Petrenko, A., Lefèvre, D., and Moutin, T.: Longitudinal contrast in Turbulence along a ∼19S section in the Pacific and its consequences on biogeochemical fluxes, Biogeosciences Discussions, 2018, 1–33, 2018.

Caffin, M., Moutin, T., Foster, R. A., Bouruet-Aubertot, P., Doglioli, A. M., Berthelot, H., Grosso, O., Helias-Nunige, S., Leblond, N., Gimenez, A., Petrenko, A. A., de Verneil, A., and Bonnet, S.: Nitrogen budgets following a Lagrangian strategy in the Western Tropical South Pacific Ocean: the prominent role of N_2 fixation (OUTPACE cruise), Biogeosciences Discussions, 2017, 1–34, https://doi.org/10.5194/bg-2017-468, https://www.biogeosciences-discuss.net/bg-2017-468/, 2017.

Cravatte, S., Kessler, W. S., and Marin, F.: Intermediate Zonal Jets in the Tropical Pacific Ocean Observed by Argo Floats*, Journal of Physical Oceanography, 42, 1475–1485, 2012.

Cravatte, S., Kestenare, E., Marin, F., Dutrieux, P., and Firing, E.: Subthermocline and Intermediate Zonal Currents in the Tropical Pacific Ocean: Paths and Vertical Structure, Journal of Physical Oceanography, 47, 2305–2324, https://doi.org/10.1175/JPO-D-17-0043.1, 2017.

Davis, R. E.: Intermediate-depth circulation of the Indian and South Pacific Oceans measured by autonomous floats, Journal of Physical Oceanography, 35, 683–707, 2005.

de Verneil, A., Rousselet, L., Doglioli, A. M., Petrenko, A. A., Maes, C., Bouruet-Aubertot, P., and Moutin, T.: OUTPACE long duration stations: physical variability, context of biogeochemical sampling, and evaluation of sampling strategy, Biogeosciences Discussions, 2017, 1–33, https://doi.org/10.5194/bg-2017-455, https://www.biogeosciences-discuss.net/bg-2017-455/, 2017a.

de Verneil, A., Rousselet, L., Doglioli, A. M., Petrenko, A. A., and Moutin, T.: The fate of a southwest Pacific bloom: gauging the impact of submesoscale vs. mesoscale circulation on biological gradients in the subtropics, Biogeosciences, 14, 3471–3486, https://doi.org/10.5194/bg-14-3471-2017, https://www.biogeosciences.net/14/3471/2017/, 2017b.

Flierl, G. R.: Particle motions in large-amplitude wave fields, Geophysical & Astrophysical Fluid Dynamics, 18, 39–74, 1981.

Fumenia, A., Moutin, T., Bonnet, S., Benavides, M., Petrenko, A., Helias Nunige, S., and Maes, C.: Excess nitrogen as a marker of intense dinitrogen fixation in the Western Tropical South Pacific Ocean: impact on the thermocline waters of the South Pacific, Biogeosciences Discussions, 2018, 1–33, https://doi.org/10.5194/bg-2017-557, https://www.biogeosciences-discuss.net/bg-2017-557/, 2018.

Gaillard, F.: ISAS-tool version 6: Method and configuration, 2012.

Gaillard, F., Reynaud, T., Thierry, V., Kolodziejczyk, N., and Von Schuckmann, K.: In situ–based reanalysis of the global ocean temperature and salinity with ISAS: Variability of the heat content and steric height, Journal of Climate, 29, 1305–1323, https://doi.org/10.1175/JCLI-D-15-0028.1, 2016.

Ganachaud, A. and Wunsch, C.: Oceanic nutrient and oxygen transports and bounds on export production during the World Ocean Circulation Experiment, Global Biogeochemical Cycles, 16, 2002.

Gasparin, F., Ganachaud, A., and Maes, C.: A western boundary current east of New Caledonia: Observed characteristics, Deep Sea Research Part I: Oceanographic Research Papers, 58, 956–969, 2011.

Gasparin, F., Maes, C., Sudre, J., Garcon, V., and Ganachaud, A.: Water mass analysis of the Coral Sea through an Optimum Multiparameter method, Journal of Geophysical Research: Oceans, 119, 7229–7244, 2014.

IOCCG: Remote Sensing in Fisheries and Aquaculture, Forget, M.-H., Stuart, V. and Platt, T. (eds.), Reports of the International Ocean-Colour Coordinating Group, No. 8, IOCCG, Dartmouth, Canada, p. 92-95, 2009.

Las Heras, M. M. and Schlitzer, R.: On the importance of intermediate water flows for the global ocean overturning, Journal of Geophysical Research: Oceans, 104, 15 515–15 536, 1999.

Maes, C.: BIFURCATION cruise, RV Alis, https://doi.org/10.17600/12100100, 2012.

Maharaj, A. M., Cipollini, P., Holbrook, N. J., Killworth, P. D., and Blundell, J. R.: An evaluation of the classical and extended Rossby wave theories in explaining spectral estimates of the first few baroclinic modes in the South Pacific Ocean, Ocean Dynamics, 57, 173–187, 2007.

Martinez, E., Claustre, H., Rodier, M., Poteau, A., Maes, C., Mignot, A., Taquet, M., Ponsonnet, C., and Maamaatuaiahutapu, K.: THOT (TaHitian Ocean Time series) a climate oceanographic observatory in the open ocean central, 2015.

Maximenko, N. A., Bang, B., and Sasaki, H.: Observational evidence of alternating zonal jets in the world ocean, Geophysical research letters, 32, 2005.

Maximenko, N. A., Melnichenko, O. V., Niiler, P. P., and Sasaki, H.: Stationary mesoscale jet-like features in the ocean, Geophysical Research Letters, 35, 2008.

Mendoza, C. and Mancho, A. M.: Hidden geometry of ocean flows, Physical review letters, 105, 038 501, 2010.

Mitchell, B.: Resolving spring bloom dynamics in the Sea of Japan, in: ALPS: Autonomous and Lagrangian Platforms and Sensors, Workshop Report, pp. 26–27, https://geo-prose.com/pdfs/alps_report.pdf, 2003.

Moutin, T., Doglioli, A. M., de Verneil, A., and Bonnet, S.: Preface: The Oligotrophy to the UlTra-oligotrophy PACific Experiment (OUTPACE cruise, 18 February to 3 April 2015), Biogeosciences, 14, 3207–3220, https://doi.org/10.5194/bg-14-3207-2017, https://www.biogeosciences.net/14/3207/2017/, 2017.

Ollitrault, M. and Colin de Verdière, A.: The ocean general circulation near 1000-m depth, Journal of Physical Oceanography, 44, 384–409, 2014.

Ollitrault, M. and Rannou, J.-P.: ANDRO: An Argo-based deep displacement dataset, Journal of Atmospheric and Oceanic Technology, 30, 759–788, 2013.

Phillips, H. and Bindoff, N.: On the nonequivalent barotropic structure of the Antarctic Circumpolar Current: An observational perspective, Journal of Geophysical Research: Oceans, 119, 5221–5243, 2014.

Rousselet, L., Doglioli, A., Maes, C., Blanke, B., and Petrenko, A.: Impacts of mesoscale activity on the water masses and circulation in the Coral Sea, Journal of Geophysical Research: Oceans, 121, 7277–7289, 2016.

Rousselet, L., de Verneil, A., Doglioli, A. M., Petrenko, A. A., Duhamel, S., Maes, C., and Blanke, B.: Large to submesoscale surface circulation and its implications on biogeochemical/biological horizontal distributions during the OUTPACE cruise (SouthWest Pacific), Biogeosciences Discussions, 2017, 1–29, https://doi.org/10.5194/bg-2017-456, https://www.biogeosciences-discuss.net/bg-2017-456/, 2017.

Sevellec, F., Colin de Verdiére, A., and Ollitrault, M.: Evolution of Intermediate Water Masses Based on Argo Float Displacements, Journal of Physical Oceanography, 47, 1569–1586, 2017.

Webb, D. J.: Evidence for shallow zonal jets in the South Equatorial Current region of the southwest Pacific, Journal of Physical Oceanography, 30, 706–720, 2000.